Comparison of Alternative pre-mRNA Splicing and Gene Expression Patterns in Midbrain Lineage Cells Carrying Familial Parkinson's Disease Mutations

Yeon J. Lee[1,2,9,10], Khaja Syed[1,9,10], Oriol Busquets[3,9,11], Hanqin Li[1,8,9,11] Jesse Dunnack[1,9], Atehsa Sahagun[1,9], Helen S. Bateup[1,6,7,9], Frank Soldner[3,4,5,9], Dirk Hockemeyer[1,6,8,9], Donald C. Rio[1,2,9]

Affiliations:

[1] University of California, Berkeley, Molecular and Cell Biology, Berkeley, CA, 94720; [2] University of California, Berkeley, California Institute for Quantitative Biosciences, Berkeley, CA, 94720;[3] Dominick P. Purpura Department of Neuroscience, Albert Einstein College of Medicine, Rose F. Kennedy Center, Albert Einstein College of Medicine, 1410 Pelham Parkway South, Bronx, NY 10461; [4] Department of Genetics, Albert Einstein College of Medicine, 1301 Morris Park Ave., Bronx, NY 10461; [5] Ruth L. and David S. Gottesman Institute for Stem Cell and Regenerative Medicine Research, Albert Einstein College of Medicine, 1301 Morris Park Ave., Bronx, NY 10461; [6] Chan Zuckerberg Biohub, San Francisco, CA, 94158; [7] Helen Wills Neuroscience Institute, University of California, Berkeley, Berkeley, CA 94720;
[8] Innovative Genomics Institute, University of California, Berkeley, CA, 94720; [9] Aligning Science Across Parkinson's (ASAP) Collaborative Research Network, Chevy Chase, MD, 20815.

Author list footnotes:

[10,11]authors contributed equally

Corresponding authors e-mail addresses: [*]Correspondence: don_rio@berkeley.edu.

Summary

Parkinson's disease (PD) is a devastating neurodegenerative disorder, with both genetic and environmental causes. Human genetic studies have identified ~20 inherited familial genes that cause monogenic forms of PD. We have investigated the effects of individual familial PD mutations by developing a medium-throughput platform using genome-editing to install individual PD mutations in human pluripotent stem cells (hPSCs) that we subsequently differentiated into midbrain lineage cells including dopaminergic (DA) neurons in cell culture. Both global gene expression and pre-mRNA splicing patterns in midbrain cultures carrying inherited, pathogenic PD mutations in the PRKN and SNCA genes were analyzed. This analysis revealed that PD mutations lead to many more pre-mRNA splicing changes than changes in overall gene RNA expression levels. Importantly, we have also shown that these splicing changes overlap with changes found in PD patient postmortem brain sample RNA-seq datasets. These pre-mRNA splicing changes are in genes related to cytoskeletal and neuronal process formation, as well as splicing factors and spliceosome components. We predict that these mutation-specific pre-mRNA isoforms can be used as biomarkers for PD that are linked to the familial PD mutant genotypes.

Introduction

Parkinson disease (PD) affects 2-3% of individuals over 65 years of age and is the second most common neurodegenerative disease (Aarsland et al., 2021, Poewe et al., 2017). PD is characterized by severe deterioration of motor function caused by loss of dopaminergic neurons in the substantia nigra and accompanied deficient dopamine release in the caudate/putamen (Kouli et al., 2018). A hallmark of PD is the intracellular aggregation of the protein α-synuclein into histologically detectable inclusions called Lewy bodies (Aarsland et al., 2021, Poewe et al., 2017). Cells outside the brain, including cells throughout the central and peripheral autonomic nervous system are also affected as the disease progresses (Poewe et al., 2017, Mendoza-Velasquez et al., 2019, Chen et al., 2020).

Lewy body diseases include dementia with Lewy body disease (DLB) and Parkinson's disease with dementia (PDD). In PD, PDD and DLB, the protein α-synuclein abnormally accumulates in the brain in aggregates, or clumps, called Lewy bodies. Key insights into the mechanism of the disease came from human genetic studies that have identified 20 genes to cause familial monogenetically inherited forms of PD (Aarsland et al., 2021, Poewe et al., 2017). Many of these genes, including *SNCA*, which encodes α-synuclein itself, point to defects in the lysosomal-autophagy system (LAS) (Winslow et al., 2010, Navarro-Romero et al., 2020). It is known that α-synuclein oligomers can inhibit macro-autophagy, similarly to familial PD mutations in the LRRK2 protein kinase that impair the LAS (O'Hara et al., 2020). Other mutant genes linked to PD affect lysosome or mitochondrial function, as well as lipid and protein sorting (Navarro-Romero et al., 2020, Plotegher and Duchen, 2017). The underlying mechanisms of pathogenesis include defects in proteostasis, calcium homeostasis, mitochondrial and autophagy dysfunction, oxidative stress, altered axonal transport and neuroinflammation (Lehtonen et al., 2019, Wilson et al., 2023).

Dysregulated alternative pre-mRNA splicing is emerging as a new and common mechanism implicated in the pathogenesis of neurodegenerative diseases such as Alzheimer's disease, PD and spinal muscular atrophy (SMA) (Nikom and Zheng, 2023, Li et al., 2021). We have developed a platform to study the effects of familial, hereditary PD mutations on pre-mRNA splicing patterns and gene expression changes in human pluripotent stem cells (hPSCs) that can be differentiated to dopaminergic (DA) neurons *in vitro.* We have previously developed a medium-throughput genome-editing platform using Cas9 and prime editing to engineer many of the most common familial PD mutations into hPSCs (Li et al., 2022b, Busquets et al., 2024). Using cells from this resource, we examined the effects on gene expression and pre-mRNA splicing patterns caused by common familial PD mutations in the *PRKN* (parkin; PARK2; Exon 3 deletion; Ex3del) and *SNCA* (alpha-synuclein; PARK1; A30P) genes (Kruger et al., 1998, Polymeropoulos et al., 1997, Isaacs et al., 2017, Sasaki et al., 2004). Following differentiation of multiple independent cell clones carrying the *PRKN* and *SNCA* PD mutations, we carried out deep bulk short-read RNA sequencing (RNA-seq) using the Illumina platform to determine both global gene expression and pre-mRNA splicing patterns, using an annotation-free method called the Junction Usage Model or JUM for analysis and comparison of splicing patterns (Wang and Rio, 2018). We found that while the transcriptomes of cells carrying the *PRKN* Ex3del and *SNCA* (A30P) familial mutations did exhibit minor changes in gene expression levels, that there were many more changes in pre-mRNA spliced transcript isoforms in pathways relevant to PD. Moreover, comparison of our RNA-seq data to PD patient postmortem brain tissue RNA-seq data (Feleke et al., 2021) (that was obtained from patients with PD and related synucleinopathies (PD with dementia (PDD) and dementia with Lewy Bodies (DLB)) showed overlap with transcripts that are differentially spliced. Taken together, our data support the idea that the pre-mRNA splicing pattern defects we observe in hPSC-derived midbrain DA neurons (mDA) *in vitro* are relevant to PD, that these transcript isoforms may serve as useful biomarkers,

and might be amenable to RNA therapeutics (Anthony, 2022, Li et al., 2022a, Rogalska et al., 2023).

Results

Generation of dopaminergic (DA) neurons using human pluripotent stem cells (hPSCs) carrying familial PD mutations in the PRKN and SNCA genes.

To study the effects of PD-linked mutations on splicing, we have established a genome- editing platform to engineer PD mutations in hPSCs to generate isogenic stem cell models. Multiple clonally independent isogenic stem cell lines were generated carrying the familial PD mutations including *PRKN* (Ex3del) and *SNCA* (A30P) through CRISPR cas9 and prime editing techniques as previously reported (Figure 1) (Li et al., 2022b, Busquets et al., 2024). We differentiated these hPSCs into midbrain progenitor cells and dopaminergic neurons (mDA), which are the primary cell type that degenerates in PD. We derived midbrain lineage cells using a recently reported protocol (Kim et al., 2021), which generated dopamine neurons from hPSCs by boosting WNT signaling during early midbrain lineage patterning (Figure 1B). Briefly, after the initial patterning for 11 days, cells were differentiated over 3 weeks. The resulting differentiated mDA cells robustly expressed key markers TH and FOXA2 as shown in (Figure 1C) across three subclones of *PRKN* (Ex3del) and *SNCA* (A30P) mutant expressing cells. Gene expression analysis from bulk RNA seq data of the differentiated mDA cells at day 35 confirmed expression of key neuronal markers (e.g. *FOAX2*, *STMN2*, *MAP2*, Figure 1D), indicating robust differentiation within these hPSC-derived cell lines.

Global pre-mRNA splicing pattern changes linked to a familial PRKN gene exon 3 deletion (Ex3del) show changes in transcript isoforms from genes involved in cell projection organization, the cytoskeleton and regulation of neurogenesis.

During neuronal differentiation, alternative splicing modulates diverse processes such as signaling activity, centriolar dynamics, and metabolic pathways (Su et al., 2018). RNA-seq data

can provide insights into the regulation of alternative splicing by revealing the usage of known or unknown (unannotated) splice sites as well as the expression level of exons. Using 35 day-differentiated mDA cells derived from human pluripotent stem cells (hPSCs) carrying either the *PRKN* Exon 3 deletion (Ex3del, Supplemental Figure S1I) or wild-type genotypes, we prepared total RNA, polyA$^+$-selected it and then generated random-primed cDNA libraries from 3 independently derived cell clones in technical triplicates. These libraries were sequenced on the Illumina NovaSeq S4 platform with between 200-300M paired-end 150bp (PE150) reads. The large datasets coming from this experiment were analyzed using the Junction Usage Model (JUM) algorithm and software (Wang and Rio, 2018) to compare and quantitate pre-mRNA splicing pattern differences between the *PRKN* mutant and wild-type cells. The ratio between reads including or excluding exons, also known as percent spliced in index (PSI), indicates how efficiently sequences of interest are spliced into transcripts. By comparing data from the three *PRKN* mutant cell clones to three wild-type clones, with the PSI cut-off set to > 5%, we observed thousands of splicing events that differed between the wild-type and mutant cell lines, mostly in the category that JUM denoted as “composite”, which is a combination of splicing patterns beyond a simple splicing event within the same splicing structure (Figure 2A). In *PRKN* mutant cells, we found that there was differential splicing of over 1,119 genes, found in at least two of the three *PRKN* (Ex3del) mutant cell clones compared to wild-type cells (Figure 2B). Analysis of these transcripts grouped by gene ontology (GO) terms indicated that these genes clustered in cell projection organization including the cytoskeleton, regulation of cell projection organization and the regulation of neurogenesis (Figure 2C). Taken together, we found thousands of pre-mRNA splicing pattern changes that were found only in the *PRKN* mutant cells. Looking for overlap in patterns of RNA processing defects in the other familial mutant cell lines carrying PD mutations should identify common genes and transcript isoforms prominently linked to PD.

Global differential gene expression profiling in 35 day-differentiated mDA cells with the PRKN (Ex3del) mutation compared to control wild-type cells.

Using the RNA-seq data from the *PRKN* (Ex3del) mutant and wild type cells, we next analyzed overall gene expression (RNA transcript levels) using DESeq2 (Love et al., 2014). This analysis showed that there were 460 genes (fold change (FC) > 1.5, FDR-adjusted p-value < 0.05) that were differentially expressed between the *PRKN* mutant and wild type cells (Figure 3A). The 337 up-regulated genes were linked by GO terms to neuronal differentiation and cell signaling (Figure 3B, top, left). Gamma-Aminobutyric Acid Type A Receptor Subunit Alpha3 (*GABRA3*) variants are associated with epileptic seizures, encephalopathy and dysmorphic features (Niturad et al., 2017), and 2 novel rare variants of teneurin transmembrane protein 1 (*TENM4*) were found in a Chinese cohort of sporadic PD patients (Pu et al., 2020). These two genes were upregulated in the *PRKN* mutant cells (Figure 3B, top, right). The 123 down-regulated genes were linked to secretory pathways, cell differentiation and calcium transport regulation (Figure 3B, bottom, left). Note that two genes, *IGF1*, insulin-like growth factor 1, which can regulate glucose transport and glycogen synthesis and *CHRNA5*, a cholinergic receptor nicotinic alpha 5 subunit, which is a member of a superfamily of ligand-gated ion channels that mediate fast signal transmission at synapses, were both down-regulated in the *PRKN* mutant cells (Figure 3B, bottom, right). A study indicated plasma IGF-1 levels can be used to assess the probability that PD patients have non-motor symptoms, such as cognitive dysfunction, anxiety and depression (Shi et al., 2022). The differential expression of these genes in the *PRKN* mutant cells could alter the cellular physiology of the mDA cells. Interestingly, there are more pre-mRNA splicing changes than gene expression changes in the *PRKN* (Ex3del) mutant cells compared to wild-type. This result is relevant because it has been shown that alternative splicing in the nervous system often results in mRNA isoforms that encode proteins with altered protein-protein interactions (Ellis et al., 2012).

Global pre-mRNA splicing pattern changes linked to a familial SNCA gene point mutation (A30P) reveal changes in transcript isoforms from genes involved in cell projection organization, the cytoskelton and regulation of neurogenesis.

Using the same pipeline as for *PRKN* mutant mDA cells, we compared midbrain DA neuronal cells carrying either the *SNCA* (A30P) mutant or wild type genotypes. Total RNA was isolated, enriched for the polyadenylated (poly A^+)-RNA and then generated random-primed cDNA libraries from three independently derived cell clones in technical triplicates. As before, these libraries were sequenced on the Illumina NovaSeq S4 platform to between 200-300M PE150 reads. The large datasets were analyzed using the Junction Usage Model (JUM) (Wang and Rio, 2018) to compare and quantitate pre-mRNA splicing pattern differences between the *SNCA* mutant and wild type cells. We detected thousands of differentially spliced gene transcripts in the *SNCA* (A30P) mutant cells compared to wild type cells, with at least delta PSI of 5% or higher. Mostly these differential pre-mRNA splicing events fell into a composite pattern category, which is a unique property of JUM analysis, which can depict complex splicing events that occur within the same splicing structure (Wang and Rio, 2018), followed by alternative 5' splice site (A5SS) and alternative 3' splice site (A3SS) (Figure 4A). By comparison of the *SNCA* mutant and wild type cell line data, we found that there was differential splicing in transcripts derived from 1,957 genes, that were found in at least two of the three *SNCA* mutant cell clones (Figure 4B). Analysis of these transcripts grouped by gene ontology (GO) terms indicated that the genes encoding these transcript isoforms were clustered in cell projection organization including the cytoskeleton, regulation of cell projection organization, the regulation of neurogenesis and regulation of GTPase activity (Figure 4C). The finding of a link to GTPase activity is interesting given the prominent role of the Rab proteins as substrates for the LRRK2 kinase and the ciliary defects characteristic of PD (Pfeffer, 2023, Pfeffer, 2018, Dhekne et al., 2018). Taken together and given the isogenic nature of the cells, we find almost 2,000 pre-mRNA splicing pattern changes that are found only in the *SNCA* (A30P) mutant cells. Looking

for overlap in patterns of RNA processing defects in the other familial mutant cell lines should identify common genes and transcript isoforms prominently linked to PD.

Analysis of global differential gene expression in 35 day-differentiated dopaminergic (DA) neurons with the SNCA (A30P) mutation compared to wild-type mDA cells.

Using the RNA-seq data from the *SNCA* (A30P) mutant and wild-type cells, we next analyzed overall gene expression (RNA transcript levels) using DESeq2 (Love et al., 2014). This analysis showed that there were 619 genes (fold change (FC) > 1.5, FDR-adjusted p-value < 0.05) that were differentially regulated between the *SNCA* (A30P) mutant and wild-type cells (Figure 5A). The 446 up-regulated genes were linked by GO terms to glutamate receptor and neurotransmitter receptor signaling (Figure 5B, top, left). Note that two genes, *CHL1*, Cell Adhesion-Like Molecule 1 and *UNC13A*, a member of the *UNC13* gene family, are known to bind to phorbol esters and diacylglycerol and play important roles in neurotransmitter release at synapses (Willemse et al., 2023). Both of these genes are upregulated in the *SNCA* (A30P) mutant cells (Figure 5B, top, right). *CHL1* promotes insulin secretion and negatively regulates the proliferation of pancreatic beta cells (Jiang et al., 2020). A close homolog of L1-deficiency ameliorates inflammatory bowel disease by regulating the balance of Th17/Treg immune T cells (Yao et al., 2020). Dendritic spine and excitatory synapse density of pyramidal neurons in the developing neocortex is known to be regulated by *CHL1* (Mohan et al., 2019). Single nucleotide polymorphisms in the *UNC13A* gene are associated with sporadic amyotrophic lateral sclerosis (ALS) (Placek et al., 2019). *UNC13A* provides a novel link between ALS and frontotemporal lobar dementia (FTLD) and identifies changes in neurotransmitter release and synaptic function as a converging mechanism in the pathogenesis of these neurodegenerative disorders. It is also known that cryptic exon splicing of *UNC13A* plays a major role in the pathogenesis of ALS and FTLD-TDP (Mehta et al., 2023, Lipstein, 2022, Ma et al., 2022, Brown et al., 2022), as well as Alzheimer's disease (Agra Almeida Quadros et al., 2024). Given our results, it is possible UNC13A may play similar role in PD.

The 173 down-regulated genes were linked to secretory pathways, neuronal differentiation and calcium transport regulation (Figure 5B, bottom, left). *CADPS2*, a member of the calcium-dependent activator of secretion (CAPS) protein family (Shinoda et al., 2011), which are calcium binding proteins that regulate the exocytosis of synaptic and dense-core vesicles in neurons and neuroendocrine cells. ZNF473 encodes a member of the Krueppel C_2H_2-type zinc-finger (ZNF) protein family. *ZNF473* is a component of the U7 small nuclear ribonucleoprotein (snRNP) complex that plays a role in histone 3'-end messenger RNA processing and may be required for cell cycle progression to S phase. Numerous studies have shown that many ZNF family proteins are associated with neurological diseases (Bu et al., 2021). A lower expression of the *ZNF473* gene in the SNCA (A30P) mutant mDA cells may lead to aberrant alternative splicing and cell cycle dysregulation. Previous exon microarray studies revealed alternative splicing alterations in PD patients (Soreq et al., 2012, Potashkin et al., 2012, Santiago et al., 2013) and cell cycle dysregulation has been implicated in the pathogenesis of neurodegenerative disorders, including PD (Joseph et al., 2020). Thus, both of these interesting genes may play significant roles in PD physiology due to the *SNCA* (A30P) mutation. It is important to emphasize that there are more changes at the RNA processing level than gene expression/RNA level in our datasets, reinforcing the idea that RNA splicing is an important process for specifying cell type identity and diversification in the brain (Li et al., 2021).

Overlap of differential pre-mRNA transcript spliced isoform expression between PD patient brain (anterior cingulate cortex) postmortem data with the data from hPSC-derived mDA cells carrying familial PRKN (Ex3del) and SNCA (A30P) mutations.

Recently, Mina Ryten's group published a bulk-tissue RNA-sequencing dataset (Feleke et al., 2021) that contains 24 postmortem human brain cortex samples with 19 patients with different Lewy body diseases including PD, PDD, and DLB with 5 control individuals without any

neurological condition. The Ryten group used Leafcutter (Li et al., 2018) for alternative splicing pattern analysis and determined 305 PD-associated genes had splicing pattern changes (Feleke et al., 2021). Leafcutter uses an intron-centric view of splicing and therefore all detected splicing events are given as intron coordinates in split-read clusters. It defines AS events as clusters of overlapping introns which may involve multiple alternative 3' and 5' splice sites and skipped exons, making it hard to determine the actual patterns and modes of alternative splicing used by specific splicing junctions. Hence, we took the Ryten lab's raw data (which was deeply sequenced at 150-250 million PE150 Illumina reads) and analyzed the data using JUM (Wang and Rio, 2018), which allows us to determine AS modes and patterns, while yielding a quantitatively comparing PSI values for usage of all detected splice junctions.

We compared the Ryten lab postmortem brain cortex data analyzed by either JUM or Leafcutter (Figure 6). Because JUM and Leafcutter use different algorithms for splicing pattern analysis, as well as different cutoffs for statistical analysis, there was some overlap but also differences in terms of the number of differentially spliced transcripts between the software programs (Figure 6A). While there were slightly fewer splicing changes found by JUM in the PD patient data, the general trend was the same, in which the most differential splicing events identified in our cell models were observed in patients with DLB compared to PD or PDD (Figure 6A). This shows alternative splicing is an important mechanism in the development of Lewy body diseases, including PD and can be used to distinguish these three clinically distinct Lewy body diseases.

We next compared splicing pattern changes identified by JUM in *PRKN* (Ex3del) and *SNCA* (A30P) mutant mDA cells, we also compared those splicing changes to those previously reported by the Ryten group (Feleke et al., 2021), who carried out RNA-seq analysis on postmortem samples from PD and control patient brain samples (Feleke et al., 2021) (Figure 6B). There were 21 common genes whose transcript isoforms changed and overlapped between the *PRKN* (Ex3del) mutant cells and the PD patient brain sample data (Figure 6B, top,

right box) and 37 common genes whose transcript isoforms changed and overlapped between the *SNCA* (A30P) mutant cells and the PD patient biopsy data (Figure 6B, bottom, right box). Interestingly, this included splicing factors including RBFOX1, DDX46 and SRRM2 whose transcript splicing patterns were altered in both the PD patient brain samples and the hPSC-derived mDA cells. These changes in splicing factor isoforms could also lead, either directly or indirectly, to aberrant splicing of multiple pre-mRNAs. We analyze both SRRM2 and DDX46 in more detail below, but it is interesting to note that SRRM2 was identified as a splicing factor whose pre-RNA was aberrantly spliced in PD patients prior to the advent of high-throughput cDNA sequencing technologies (Fu et al., 2013, Shehadeh et al., 2010).

Transcripts from the pre-mRNA splicing factors DDX46 and SRRM2 are differentially spliced in PRKN (Ex3del) mutant mDA cells.

We found two genes of particular interest whose transcript splicing patterns were altered in the *PRKN* (Ex3del) mutant mDA cells. These two genes were *SRRM2* and *DDX46*. SRRM2 is a well-known pre-mRNA splicing factor, and consistent with our observations, dysregulation of the RNA splicing factor SRRM2 was previously observed in PD patients (Shehadeh et al., 2010, Fu et al., 2013). More recently SRRM2 has been linked to neurodevelopmental disorders (Regan-Fendt et al., 2023) and inflammation (Cui et al., 2023). The *DDX46* gene, and its yeast homolog prp5, are known RNA helicases and critical protein components of the spliceosomal U2 small nuclear ribonucleoprotein (snRNP) which plays a role in intron branchpoint recognition (Kastner et al., 2019, Plaschka et al., 2019, Will and Luhrmann, 2011).

Relevant for PD, *DDX46* has been found within a GWAS interval linked to PD, locus 28 with the index variant rs11950533 from a recent PD GWAS study (Bressan et al., 2023). Our analysis indicates that the *DDX46* pre-mRNA splicing pattern is altered in the *PRKN* (Ex 3del) mutant mDA cells (Figure 7A). Interestingly, quantitative analysis of DDX46 protein levels in the *PRKN* (Ex3del) mutant mDA cells shows reduced protein DDX46 levels at day 11 of differentiation and

elevated DDX46 protein levels at day 40 of differentiation (Figure 7B). These variations in DDX46 protein levels could affect the action of U2 snRNP to modulate alternative splicing in the mutant mDA cells and could be linked to PD symptoms.

We next wanted to validate changes in alternative pre-mRNA splicing patterns found in the RNA-seq data using quantitative reverse-transcription polymerase chain reaction (RT-PCR). In these experiments, we used analysis of *GAPDH* mRNA as a positive control that should not vary in these experiments. We found alterations in the levels of spliced mRNAs in two regions of the *DDX46* gene, denoted A and B (Figure 7C). We also found alterations in splicing patterns for the *MARK4* (microtubule affinity-regulating kinase 4), *CAMPSAP2* (calmodulin-regulated spectrin-associated protein family member 2) and *MFSD6* (major facilitator superfamily domain-containing 6) genes (Figure 7C). These results confirm that our analysis of pre-mRNA splicing patterns in *PRKN* (Ex3del) mutant cells are altered compared to wild-type cells and that pre-mRNAs derived from genes linked to the cytoskeleton are affected (see Figure 2).

Discussion

Parkinson disease (PD) is the second most prevalent neurodegenerative disease. There is no cure and the mainstay (or standard) treatment is to administer L-DOPA. Generally, the problem with l-DOPA is that efficacy wanes after chronic use and that is when side effects like dyskinesia can occur (Kwon et al., 2022, Dias et al., 2023). There are only limited PD biomarkers available for screening (e.g. α-synuclein seeding amplification assay, (Concha-Marambio et al., 2023, Fernandes Gomes et al., 2023)) to detect the condition before symptoms develop. Intensive research is underway to uncover the underlying biochemical and cell biological mechanisms that will lead to new fundamental insights and information to allow the development of early detection and therapeutic interventions (Schekman and Riley, 2019).

As is the case for other neurodegenerative diseases, like amyotrophic lateral sclerosis (ALS) and spinal muscular atrophy (SMA), defects in protein homeostasis, aggregation, RNA binding proteins and RNA processing lead to pathologic physiological changes in PD (Brinegar and Cooper, 2016, Conlon and Manley, 2017, Mann and Donnelly, 2021). Identifying RNA processing events and pre-mRNA splicing events linked to these disease states has led to identification of target disease-relevant transcripts for therapeutic interventions using antisense oligonucleotides (ASOs) (Bennett et al., 2019, Meyer et al., 2020), small molecules (Meyer et al., 2020), and gene therapy (Li et al., 2023). Given the advances in the delivery of nucleic acid therapeutics (Damase et al., 2021) and messenger RNA (Huang et al., 2022), it is likely that once key RNA level targets are identified for PD, therapeutic interventions can be developed. The platform developed and outlined here utilizing hPSCs will play an important role in the development of PD therapeutics.

It is clear that for other diseases, such as a variety of cancers, including blood cancers like myelodysplastic syndrome (MDS), and neurodegenerative diseases like SMA, Huntington disease (HD) and ALS, that mutations in RNA binding proteins and known pre-mRNA splicing factors and specific splicing events can play causative roles in the disease states and are now successful therapeutic targets (Gebauer et al., 2021, Kapeli et al., 2017). Many neurodegenerative disease states involve changes in proteostasis, mitochondrial, lysosomal and other metabolic and cell biological pathways (Wilson et al., 2023, Jagtap et al., 2023). In many cases, protein aggregation, for instance the TDP-43 protein in ALS and in PD α-synuclein aggregates are key indicators of disease. In the case of ALS, two key RNA processing events involving the Stathmin-2 (*STMN-2*) (Baughn et al., 2023) and *UNC13A* (Brown et al., 2022, Ma et al., 2022, Lipstein, 2022) genes are targets for therapeutic interventions. In addition, splicing alterations in *STMN-2* and *UNC13A* have recently been found in Alzheimer's disease patients (Agra Almeida Quadros et al., 2024).

Here, we have developed a system to investigate RNA-level changes that are linked to the 20 most common familial PD hereditary genes, such as *PRKN*, *SNCA* and *LRRK2* (Poewe et al. 2017). Our results linking splicing pattern alterations to PD are consistent with uncovered defects in global pre-mRNA splicing patterns discovered in other neurodegenerative diseases such as ALS (Li et al., 2021, Wang et al., 2020), SMA (Singh and Singh, 2018) and various cancers (Choi et al., 2023, Zhang and Manley, 2013, Bradley and Anczukow, 2023, Stanley and Abdel-Wahab, 2022, El Marabti and Abdel-Wahab, 2021). It is also clear that mutations in RNA binding protein genes, such as TDP-43 (Nussbacher et al., 2019, Kapeli et al., 2017) and spliceosome components, such as U2AF1 and SF3B1 (Choi et al., 2023, Bradley and Anczukow, 2023, Stanley and Abdel-Wahab, 2022, El Marabti and Abdel-Wahab, 2021) play roles in neurodegeneration and cancer, respectively.

One important findingfrom this work is that in the PD mutant cells there are many more RNA splicing changes than gene expression level changes in the hPSC-derived mDA cells. This conclusion is supported by RNA-seq data from PD patient postmortem brain samples (Feleke et al., 2021), which overlap with some of the splicing pattern changes found in our RNA-seq analysis of hPSC-derived mDA cells carrying familial PD mutations. In our initial studies with the familial *SNCA* and *PRKN* mutants, we have identified splicing pattern changes for the well-known RNA splicing factors RBFOX1, SRRM2, and DDX46. These changes could lead to a cascade of pre-mRNA splicing defects, since many pre-mRNAs require these factors for correct processing. Interestingly, the DDX46 gene that encodes a known component of the spliceosome and whose splicing patterns were in our experiments and and in PD patient brain samples, resides in one of the new GWAS regions identified in a recent study (Bressan et al., 2023). We showed here that *DDX46* pre-mRNA splicing is altered in the *PRKN* (Ex3del) mutant mDA cells and that the protein is upregulated in the differentiated mDA cells. Thus, the platform we have developed will enable the identification of common defects in RNA processing patterns

and RNA splicing factors that occur in mDA cells derived from hPSCs engineered with other PD familial mutations (Busquets et al., 2024).

Conflict of Interests:

The authors declare that they have no conflict of interest.

Acknowledgments:

This work was funded by Aligning Science Across Parkinson's (ASAP-024409, ASAP-000486) through the Michael J. Fox Foundation for Parkinson's Research (MJFF). For the purpose of open access, the author has applied a CC-BY public copyright license to the Author Accepted Manuscript version arising from this submission. This work was funded entirely by the Aligning Science Against Parkinson's (ASAP) through the Michael J. Fox Foundation (MJFF); ASAP-000486). Illumina RNA sequencing was carried out at the U.C., Berkeley QB3 Coates Genome Sequencing Laboratory (GSL), supported by National Institutes of Health (NIH) S10 Instrumentation grants S10RR025622, S10RR029668, and S10RR027303.

Author Contributions:

D.H., F.S., H.S.B and D.C.R. supervised the study; Y.J.L. performed RNA isolation and RNA-seq library preparation, performed RNA-seq data analysis for bulk-RNA sequencing experiments to detect differential gene expression and bioinformatic alternative splicing analyses and gene expression. Y.J.L. performed RT-PCR validation experiments and Western-blot analysis to confirm differential expression in 35-day DA neuronal cells expressing the *PRKN* (Ex3del) and *SNCA* (A30P) mutant genes, analyzed data and generated Figures 1F-H, 2-7. K.M.S established the hPSC differentiation system and performed dopaminergic differentiations from genome-edited lines, and generated Figure 1A-1E. H.L, O.B, J.D established the *PRKN* and *SNCA* mutant cell lines. K.M.S and A.S performed immunostaining and qPCRs on the

midbrain dopaminergic cells. Y.J.L. and D.C.R. wrote the initial draft of the manuscript. All authors contributed to and edited the final manuscript.

Figure Titles and Legends

Figure 1. Platform for the medium-throughput genome-editing of human pluripotent stem cells (hPSCs) carrying relevant familial Parkinson's mutations and differentiation of these cells to midbrain lineage cells. **A)** Schematic diagram of editing pipeline and expansion into clonal hPSC lines. **B)** Schematic representing the workflow of dopamine neuron generation from hPSCs and identification of transcript isoforms using JUM. **C-D)** Immunofluorescence staining and quantification of percentage of mDA cells expressing TH and FOXA2 at day 35 of differentiation. Each point on the graph represents a subclone and error bars represent S.E.M for independent subclone quantifications. Scale bars represent 100 μm. **F-H)** Normalized gene counts for neuronal markers including *FOXA2* (forkhead box A2), *STMN2* (stathmin-2), MAP2 (microtubule-associated protein 2), in 35d differentiated edited wild-type (Ewt), *PRKN* (Ex3del) mutant, or *SNCA* (A30P) mutant cells, in comparison to undifferentiated WIBR3 hPSCs.

Figure 2. The 1,119 high-confidence differentially spliced genes in mDA neuronal cells expressing the *PRKN* Exon 3 deletion (Exon3del) mutant gene are involved in regulation of cell development, regulation of cell projection organization, regulation of neurogenesis. A) Differential alternative splicing (AS) events detected upon *PRKN* exon 3 deletion in differentiated dopaminergic (DA) neuronal cells (35d). Over 1,100 splicing events were significantly altered in the *PRKN* exon 3 deletion mutant samples in mDA neuronal cell line versus the edited wild type control (Ewt) (with $p < 0.05$, ΔPSI >5). Shown on the y-axis is the number of differential splicing events and difference in percentage spliced in (PSI) shown on the x-axis. The splicing events were filtered based on the delta (Δ)PSI. **B)** Comparison of genes

that are differentially spliced in 3 different clonal lines *PRKN* (Exon3del) mutant. This analysis using JUM results in 1,119 high confidence differentially spliced genes. **C)** A graph of the Gene Ontology (GO) term enrichment of 1,119 differentially spliced transcripts in *PRKN* (Exon3del) mutant protein-expressing mDA neuronal cells against the edited wild type control.

Figure 3. Differential gene expression analysis comparing 35-day differentiated dopaminergic (DA) neurons and progenitor cells derived from *PRKN* and *SNCA* familial mutant cells to the edited wild type (Ewt) cells. A) DESeq2 gene expression level analysis was performed to determine differentially expressed genes that are either that are down-regulated (in red) or up-regulated (in blue) in PD mutant versus wild type mDA neuronal cells with a log-fold change (FC) > 1.5 and an FDR-adjusted p-value < 0.05. **B)** A total of 460 genes were differentially expressed. The most enriched Gene-Ontology (GO) terms for the differentially expressed genes are listed for the 337 up-regulated genes; panel B (top) and the 123 down-regulated genes; panel B (bottom). **C)** A Venn diagram showing that there is a minimal overlap between differentially-spliced (DS) genes (red) and differentially-expressed (DE) genes (blue) in the 35-day differentiated mDA-neuronal cells compared to the edited wild type (Ewt) cells.

Figure 4. The 1,957 high-confidence differentially spliced pre-mRNAs in dopaminergic (DA) neuronal cells expressing the *SNCA* (A30P) mutant gene are involved regulation of cell projection organization, regulation of neurogenesis, and regulation of GTPase activity. A) A graph showing the differential alternative splicing (AS) events detected in RNA samples from *SNCA* (A30P) mutant gene-expressing mDA neuronal cells (35d) using JUM (Wang and Rio, 2018). Thousands of splicing events were significantly altered in the *SNCA* (A30P) mutant gene-expressing mDA neuronal cells versus the edited wild type control cells (Ewt) (with $p < 0.05$, ΔPSI >5). Shown on the y-axis is the number of differential splicing events and the differences in percentage spliced in (delta ΔPSI) are shown on the x-axis. The splicing

events were filtered based on the delta PSI. **B)** Comparison of genes that are differentially spliced in 3 different clonal lines *SNCA* (A30P) mutant resulted in 1,957 high confidence differentially spliced genes. **C)** A graph showing the Gene Ontology (GO) term enrichment of within the 1,957 differentially spliced transcripts in *SCNA* (A30P) mutant gene-expressing mDA neuronal cells against the edited wild type (Ewt) control indicates these genes are involved in cell projection organization, neurogenesis regulation and GTPase regulation.

Figure 5. Differential expression analysis comparing 35-day differentiated dopaminergic (DA) neuronal cells expressing the *SNCA* (A30P) mutant gene compared to the edited wild type (Ewt) cells. A) DESeq2 analysis was performed to determine differentially expressed genes that are either that are down-regulated (in red) or up-regulated (in blue) with a log fold change (FC) > 1.5 and an FDR-adjusted p-value < 0.05. A total of 619 genes are differentially expressed in mDA neuronal cells expressing *SNCA* (A30P) mutation compared to the edited wildtype cells. **B)** The most enriched Gene-Ontology (GO) terms for the differentially expressed genes are listed for 446 up-regulated genes (B) and 173 down-regulated genes. **C)** A Venn diagram showing there is a minimal overlap between differentially spliced (DS) genes (red) and differentially expressed (DE) genes (blue) in 35-day differentiated mDA neuronal cells expressing the *SNCA* (A30P) mutant gene compared to the edited wild type (Ewt) cells.

Figure 6. Comparison of differentially spliced pre-mRNAs between Parkinson disease (PD), Parkinson Disease with dementia (PDD) and Dementia with Lewy bodies (DLB) and control patient brain (anterior cingulate cortex) data and data generated from the 35-day-differentiated dopaminergic (DA) hPSC-derived neuronal cells bearing either the *PRKN* Exon 3 deletion or *SNCA* (A30P) mutations. A) Comparison of PD patient brain cortex data (Feleke et al., 2021) analyzed by either JUM (Wang and Rio, 2018) or Leafcutter (Li et al., 2018). The highest prevalence of differential alternative splicing was observed in patients with

Dementia with Lewy Bodies (DLB), by both JUM and Leafcutter software. **B)** A Venn diagram showing comparisons of differentially spliced pre-mRNAs between patient brain (anterior cingulate cortex) data and the data generated from the 35-day-differentiated mDA neuronal cells bearing either the *PRKN* (Ex3del) or *SNCA* (A30P) mutations.

Figure 7. The transcripts from the *DDX46* and *SRRM2* genes are differentially spliced in midbrain DA neuronal cells expressing the *PRKN* (Ex3del) mutation. A) Schematic diagrams of the differentially spliced regions from the *DDX46* and *SRRM2* genes. **B)** The DDX46 protein levels were determined by immunoblotting of DA neuronal cell extracts expressing either the edited wild type (Ewt) and *PRKN* (Ex3del) mutant genes that were differentiated for either 11 days or 40 days. Upregulation of the DDX46 protein detected by immunoblotting was observed in differentiated *PRKN* (Ex3del) mutant cell extracts compared to the wild type (Ewt) controls (at day 40). **C)** RT-PCR validation of several differential splicing events of the *DDX46*, *MARK4* (microtubule affinity regulating kinase 4), *CAMPSAP2* (calmodulin regulated spectrin associated protein family member 2) and *MFSD6* (major facilitator superfamily domain containing 6) pre-mRNAs in the *PRKN* (Ex3del) mutant cells.

STAR ★ METHODS

Detailed methods are provided in the online version of this paper and include the following:

- KEYRE SOURCES TABLE
- RESOURCE AVAILABILITY
  - Lead contact
  - Materials availability
  - Data and code availability
- METHOD DETAILS
  - WIBR3-hESCs derived DA neuron differentiation:
  - Immunohistochemistry:
  - RNA extraction and qRT-PCR for DA neuronal differentiation:
  - Western blot analysis
  - RT-PCR validation for splicing analysis
  - RNA-seq library preparation and sequencing
  - Analysis of pre-mRNA splicing patterns using JUM and differential expression analysis using DESeq2

KEY RESOURCES TABLE

REAGENT or RESOURCE	SOURCE	IDENTIFIER
Antibodies		
beta actin	Sigma	A2228
DDX46	Proteintech	16927-1-AP
TH	Pelfreeze	P60101
FOXA2	Abcam	Ab60721

Chemicals and Reagents		
RNeasy Minikit	Qiagen	74104
QIAshredder	Qiagen	79654
NEBNext® Poly(A) mRNA Magnetic Isolation Module	New England Biolabs	E7490
NEBNext Ultra Directional RNA Library Preparation Kit for Illumina	New England Biolabs	E7420S
NEBNext Ultra II Directional RNA Library Prep Kit for Illumina	New England Biolabs	E7760S
NEBNext Multiplex Oligos	New England Biolabs	E7335S, E7500
mTSER-plus Medium	Stem cell Technologies	100-0276
Neurobasal Medium	ThermoFisher Scientific	21103049
B27 Supplement	ThermoFisher Scientific	12587010
N2 Supplement	ThermoFisher Scientific	17502048
L-Glutamine	Sigma	G8450
Penicillin-Streptomycin	ThermoFisher Scientific	15140122
Y-27632 Dihydrochloride Rock inhibitor	Chemdea	CD0141
iMatrix-511	Takara	T304
DPBS (No calcium, No magnesium	ThermoFisher Scientific	SH30028
Accutase	Innovative Cell Technologies	AT104
Matrigel	Corning	354230
Poly L Ornithine	Sigma	P3655
Cultrex Laminin	R&D Systems	3400-010-02
LDN	Stemgent	04-0074

SHH	R&D Systems	1845-SH-100
SB431542	SelleckChem	S1067
CHIR99021	Tocris	4423
GDNF	Peprotech	450-10
BDNF	Peprotech	450-02
Dibutyryl-cAMP (Bucladesine)	Selleckchem	S7858
Sodium L-Ascorbate	Sigma	A40-34
TGFb3	R&D Systems	8420-B3-005
DAPT	Tocris	2634
Software and Algorithms		
JUM.2.0.2		Wang and Rio 2018
cufflinks.v2.1.1		Trapnell et al. 2009
STAR_2.5.3a		Dobin et al. 2013
HTSeq		Anders et al. 2015
DESeq2		Love et al. 2014

CONTACT FOR REAGENT AND RESOURCE SHARING:

Email contact for further information and reagent and resource sharing: don_rio@berkeley.edu and hockemeyer@berkeley.edu.

METHOD DETAILS

Materials availability

All unique/stable reagents generated in this study are available from the Lead Contract without restriction.

DATA AND SOFTWARE AVAILABILITY

The data reported will be deposited in the Gene Expression Omnibus (GEO) database upon the acceptance of the manuscript.

Publicly available WIBR3 hESCs RNA-seq data was downloaded (GEO accession numbers: GSM3069316, GSM3069317, GSM3069324, GSM3069325) for comparison to Ewt, *PRKN* (Ex3del) mutant and *SNCA* (A30P) mutant cells for expression of neuronal genes in differentiated cells.

METHOD DETAILS

WIBR3-hESCs derived DA neuron differentiation:

WIBR3 hESCs (passage 25-30) were maintained and grown on iMatrix-511 (Takara, T303) coated 6-well plates in mTESR plus media (Stem Cell Technologies, 100-0276). For DA neuron differentiation, the hESCs were dissociated into single cells and seeded on matrigel (Corning, 356231) coated plates with Rock inhibitor (Chemdea CD0141) at 10 μM to initiate the differentiation. We followed the recently published protocol (Kim et al., 2021) with slight modifications. Briefly, single cell suspension of hESCs were maintained with Neurobasal N2/B27 (ThermoFisher, 21103049) media containing 2 mM glutamine (Sigma, G8450) with 200 ng/ml SHH C25II (R&D Systems, 1845-SH-100) 250 nM LDN (Stemgent, 04-0074) ,10 μM SB431542 (SelleckChem, S1067), 0.7 μM CHIR99021 (Tocris, 4423) on day 1 of differentiation. On day 4, CHIR concentration was increased to 7.5 μM and on day 7 LDN, SB, SHH were removed and media was supplemented with only CHIR. On day 10, media was changed to Neurobasal B27 with 2 mM glutamine supplemented with 20 ng/ml BDNF (Peprotech, 450-02),

20 ng/ml GDNF (Peprotech, 450-10), 200 μM ascorbic acid (AA) (Sigma, A40-34), 500 μM dbcAMP (SelleckChem, S7858) and 1 ng/ml TGFb3 (R&D Systems, 8420-B3-005). On Day 11, cells were dissociated with Accutase (ThermoFisher, 00-4555-56) and split into a 1:2 or 1:4 ratio and replated on Poly L Ornithine (PLO; 30 ug/ml; Sigma, P3655), Cultrex laminin (1 ug/ml; R&D Systems, 3400-010-02) coated plates and maintained in maturation media containing BDNF, GDNF, TGFb3, AA, DAPT from day 12. On day 16, cells were dissociated with Accutase (ThermoFisher, 00-4555-56) and replated at desired high density (1-2x10^6 cells per well of 12 well plate) depending on cell growth and maintained in maturation medium (at this stage cells were cryopreserved in serum free cryopreservation media cell banker 2 (Amsbio, 11914) and thawed as per the experiment). On day 25, cells were dissociated with Accutase (ThermoFisher, 00-4555-56) and replated at higher density (> 1x10^6 cells per of 12 well plate until the experiment. On day 35, cells were lysed in the RLT lysis buffer using Qiagen kit (RNeasy, 74104) and RNA was isolated for bulk RNA sequencing.

Immunohistochemistry:

Day 35+ cells were fixed in 4% Paraformaldehyde (PFA) (ThermoFisher, J11943.K2) in 12 well plates for 15 min at room temperature (RT). PFA was discarded and subsequently cells were washed with 1X PBS (ThermoFisher, SH30028) for 10 min three times. Cells were permeabilized with 0.3% Triton X-100 (Sigma, T8787) for 15 min at RT and washed with 1xPBS for 10 min three times. Cells were blocked with 3% BSA in 1X PBS for 1 hr at RT. Cells were incubated with primary antibodies (TH (Pelfreeze,P60101; 1:1000), FOXA2 (Abcam, ab60721; 1:250)) in 3% BSA overnight at 4C. The following day, cells were washed with 1X PBS and incubated with secondary antibodies conjugated with Alexa Fluor 488 (Invitrogen, A21206; 1:500) and Alexa Fluor 594 (Invitrogen, A21207; 1:500) in 1X PBS for 1 hr at RT. The cells were washed with 1X PBS and stained with DAPI. Cells were imaged using a Zeiss AX10 Observer.A1 inverted fluorescence microscope at 10X magnification with X-cite 120Q

illuminator. Image J software was used to quantify positive cells for TH and FOXA2. Region of interest (ROIs) were manually drawn based on DAPI staining identifying the individual cells followed by with ROIs drawn for TH (around cell body) and FOXA2 (around cell nuclei) cells. Mean fluorescence intensities were measured with in the ROIs across DAPI positive cells in 3-5 different regions of the 12 well plate. A true positive staining was determined by setting a threshold at a defined fraction of average intensity of population of cells for each marker.

RNA extraction and qRT-PCR for DA neuronal differentiation:

Cells were lysed in 12 well plates and RNA was extracted using Qiagen kit. 500-1000 ng of RNA is used for cDNA synthesis using a high-capacity cDNA reverse transcription kit. Real time PCR is performed using PowerUp SYBR Green master mix in Applied Biosystems QuantStudio 6 Flex. All reactions were performed according to the manufacturer instructions. The target gene Ct values were normalized to GAPDH Ct values and gene expression is plotted as 2^-dCt values in the form of fold changes The primer sequences used are listed in table.

Western blot analysis

Lysates were prepared in RIPA buffer (50mM Tris-HCl, pH 7.4, 150mM NaCl, 1% [v/v] Nonidet P-40, 0.5% [w/v] sodium deoxycholate, 0.1% [w/v] sodium dodecyl sulfate [SDS]) containing protease inhibitors. Equivalent amounts of each sample were subjected to immunoblotting with the following antibodies: DDX46 (Proteintech, 16927-1-AP, 1:1000 dilution), beta actin (Sigma, A2228, 1:3000 dilution.

RT-PCR validation for splicing analysis

One microgram of total RNA was reverse-transcribed according to the manufacturer's instructions (Bio-Rad, 1708891) and subjected to RT–PCR with the following conditions: 30 sec at 98°C (one cycle); 10 sec at 98°C, 30 sec at 60°C, and 30 sec at 72°C (35 cycles); and 5 min

at 72°C (one cycle). RT–PCR products were resolved, visualized, and quantitated by use of an Agilent Technologies Bioanalyzer.

RNA-seq library preparation and sequencing

RNA isolation was performed using the RNeasy Minikit (Qiagen, 74104), followed by 30 min. of DNase treatment (Ambion, AM2238) at 37°C, poly(A)$^+$ RNA transcripts were isolated [NEBNext poly(A) mRNA magnetic isolation module; New England Biolabs, E7490] from 1µg of total RNA for RNA library preparation and sequencing using NEBNext Ultra Directional RNA Library Preparation Kit for Illumina (New England Biolabs, E7420S) according to the manufacturer's instruction. The samples were sequenced on an Illumina S4 with 100-bp paired-end reads at the Vincent J. Coates Genomics Sequencing Laboratory at the University of California at Berkeley.

Analysis of pre-mRNA splicing patterns using JUM and differential expression analysis using DESeq2

Pre-mRNA splicing analysis using JUM.2.0.2 software to detect pre-mRNA splicing patterns was performed as described before (Lee et al., 2018, Wang and Rio, 2018). A *P*-value of 0.05 was used as the statistical cutoff for differentially spliced AS events. Expressed genes for GO-terminology enrichment analysis was generated using cufflinks.v2.1.1(Trapnell et al., 2009) using the following parameters: --library-type fr-firststrand -m 100 -s 10, then filtered for FPKM > 1.

For Differential expression analysis, uniquely mapped reads were mapped to hg38 using STAR_2.5.3a (Dobin et al., 2013) modified version using --outFilterMultimapNmax 1. Read counts were calculated using HTSeq script htseq-count (Anders et al., 2015) with the following specifications: -s yes -r pos -f. Differential gene expression analysis was performed using DESeq2 (Love et al., 2014) using CPM cutoff. The expression cutoff (CPM) value was

determined according to the library size and normalization factors, roughly equal to $10/L$ where L is the minimum library size in millions (Chen Y, 2016).

References:

AARSLAND, D., BATZU, L., HALLIDAY, G. M., GEURTSEN, G. J., BALLARD, C., RAY CHAUDHURI, K. & WEINTRAUB, D. 2021. Parkinson disease-associated cognitive impairment. *Nat Rev Dis Primers,* 7**,** 47.

AGRA ALMEIDA QUADROS, A. R., LI, Z., WANG, X., NDAYAMBAJE, I. S., ARYAL, S., RAMESH, N., NOLAN, M., JAYAKUMAR, R., HAN, Y., STILLMAN, H., AGUILAR, C., WHEELER, H. J., CONNORS, T., LOPEZ-ERAUSKIN, J., BAUGHN, M. W., MELAMED, Z., BECCARI, M. S., OLMEDO MARTINEZ, L., CANORI, M., LEE, C. Z., MORAN, L., DRAPER, I., KOPIN, A. S., OAKLEY, D. H., DICKSON, D. W., CLEVELAND, D. W., HYMAN, B. T., DAS, S., ERTEKIN-TANER, N. & LAGIER-TOURENNE, C. 2024. Cryptic splicing of stathmin-2 and UNC13A mRNAs is a pathological hallmark of TDP-43-associated Alzheimer's disease. *Acta Neuropathol,* 147**,** 9.

ANDERS, S., PYL, P. T. & HUBER, W. 2015. HTSeq--a Python framework to work with high-throughput sequencing data. *Bioinformatics,* 31**,** 166-9.

ANTHONY, K. 2022. RNA-based therapeutics for neurological diseases. *RNA Biol,* 19**,** 176-190.

BAUGHN, M. W., MELAMED, Z., LOPEZ-ERAUSKIN, J., BECCARI, M. S., LING, K., ZUBERI, A., PRESA, M., GONZALO-GIL, E., MAIMON, R., VAZQUEZ-SANCHEZ, S., CHATURVEDI, S., BRAVO-HERNANDEZ, M., TAUPIN, V., MOORE, S., ARTATES, J. W., ACKS, E., NDAYAMBAJE, I. S., AGRA DE ALMEIDA QUADROS, A. R., JAFAR-NEJAD, P., RIGO, F., BENNETT, C. F., LUTZ, C., LAGIER-TOURENNE, C. & CLEVELAND, D. W. 2023. Mechanism of STMN2 cryptic splice-polyadenylation and its correction for TDP-43 proteinopathies. *Science,* 379**,** 1140-1149.

BENNETT, C. F., KRAINER, A. R. & CLEVELAND, D. W. 2019. Antisense Oligonucleotide Therapies for Neurodegenerative Diseases. *Annu Rev Neurosci,* 42**,** 385-406.

BRADLEY, R. K. & ANCZUKOW, O. 2023. RNA splicing dysregulation and the hallmarks of cancer. *Nat Rev Cancer,* 23**,** 135-155.

BRESSAN, E., REED, X., BANSAL, V., HUTCHINS, E., COBB, M. M., WEBB, M. G., ALSOP, E., GRENN, F. P., ILLARIONOVA, A., SAVYTSKA, N., VIOLICH, I., BROEER, S., FERNANDES, N., SIVAKUMAR, R., BEILINA, A., BILLINGSLEY, K. J., BERGHAUSEN, J., PANTAZIS, C. B., PITZ, V., PATEL, D., DAIDA, K., MEECHOOVET, B., REIMAN, R., COURTRIGHT-LIM, A., LOGEMANN, A., ANTONE, J., BARCH, M., KITCHEN, R., LI, Y., DALGARD, C. L., AMERICAN GENOME, C., RIZZU, P., HERNANDEZ, D. G., HJELM, B. E., NALLS, M., GIBBS, J. R., FINKBEINER, S., COOKSON, M. R., VAN KEUREN-JENSEN, K., CRAIG, D. W., SINGLETON, A. B., HEUTINK, P. & BLAUWENDRAAT, C. 2023. The Foundational Data Initiative for Parkinson Disease: Enabling efficient translation from genetic maps to mechanism. *Cell Genom,* 3**,** 100261.

BRINEGAR, A. E. & COOPER, T. A. 2016. Roles for RNA-binding proteins in development and disease. *Brain Res,* 1647**,** 1-8.

BROWN, A. L., WILKINS, O. G., KEUSS, M. J., HILL, S. E., ZANOVELLO, M., LEE, W. C., BAMPTON, A., LEE, F. C. Y., MASINO, L., QI, Y. A., BRYCE-SMITH, S., GATT, A., HALLEGGER, M., FAGEGALTIER, D., PHATNANI, H., CONSORTIUM, N. A., NEWCOMBE, J., GUSTAVSSON, E. K., SEDDIGHI, S., REYES, J. F., COON, S. L., RAMOS, D., SCHIAVO, G., FISHER, E. M. C., RAJ, T., SECRIER, M., LASHLEY, T., ULE, J., BURATTI, E., HUMPHREY, J., WARD, M. E. & FRATTA, P. 2022. TDP-43 loss and ALS-risk SNPs drive mis-splicing and depletion of UNC13A. *Nature,* 603**,** 131-137.

BU, S., LV, Y., LIU, Y., QIAO, S. & WANG, H. 2021. Zinc Finger Proteins in Neuro-Related Diseases Progression. *Front Neurosci,* 15**,** 760567.

BUSQUETS, O., LI, H., SYED, K. M., JEREZ, P. A., DUNNACK, J., BU, R. L., VERMA, Y., PANGILINAN, G. R., MARTIN, A., STRAUB, J., DU, Y., SIMON, V. M., POSER, S., BUSH, Z., DIAZ, J., SAHAGUN, A., GAO, J., HERNANDEZ, D. G., LEVINE, K. S., BOOTH, E. O., BATEUP, H. S., RIO, D. C., HOCKEMEYER, D., BLAUWENDRAAT, C. & SOLDNER, F. 2024. iSCORE-PD: an isogenic stem cell collection to research Parkinson's Disease. *bioRxiv***,** 2024.02.12.579917.

CHEN Y, L. A. A. S. G. 2016. From reads to genes to pathways: differential expression analysis of RNA-Seq experiments using Rsubread and the edgeR quasi-likelihood pipeline *F1000Research,* 5.

CHEN, Z., LI, G. & LIU, J. 2020. Autonomic dysfunction in Parkinson's disease: Implications for pathophysiology, diagnosis, and treatment. *Neurobiol Dis,* 134**,** 104700.

CHOI, S., CHO, N., KIM, E. M. & KIM, K. K. 2023. The role of alternative pre-mRNA splicing in cancer progression. *Cancer Cell Int,* 23**,** 249.

CONCHA-MARAMBIO, L., PRITZKOW, S., SHAHNAWAZ, M., FARRIS, C. M. & SOTO, C. 2023. Seed amplification assay for the detection of pathologic alpha-synuclein aggregates in cerebrospinal fluid. *Nat Protoc,* 18**,** 1179-1196.

CONLON, E. G. & MANLEY, J. L. 2017. RNA-binding proteins in neurodegeneration: mechanisms in aggregate. *Genes & development,* 31**,** 1509-1528.

CUI, H., DIEDRICH, J. K., WU, D. C., LIM, J. J., NOTTINGHAM, R. M., MORESCO, J. J., YATES, J. R., 3RD, BLENCOWE, B. J., LAMBOWITZ, A. M. & SCHIMMEL, P. 2023. Arg-tRNA synthetase links inflammatory metabolism to RNA splicing and nuclear trafficking via SRRM2. *Nat Cell Biol,* 25**,** 592-603.

DAMASE, T. R., SUKHOVERSHIN, R., BOADA, C., TARABALLI, F., PETTIGREW, R. I. & COOKE, J. P. 2021. The Limitless Future of RNA Therapeutics. *Front Bioeng Biotechnol,* 9**,** 628137.

DHEKNE, H. S., YANATORI, I., GOMEZ, R. C., TONELLI, F., DIEZ, F., SCHULE, B., STEGER, M., ALESSI, D. R. & PFEFFER, S. R. 2018. A pathway for Parkinson's Disease LRRK2 kinase to block primary cilia and Sonic hedgehog signaling in the brain. *Elife,* 7.

DIAS, C. M. V., LEAL, D. A. B. & BRYS, I. 2023. Levodopa-induced dyskinesia is preceded by increased levels of anxiety and motor impairment in Parkinson's disease patients. *Int J Neurosci,* 133**,** 1319-1325.

DOBIN, A., DAVIS, C. A., SCHLESINGER, F., DRENKOW, J., ZALESKI, C., JHA, S., BATUT, P., CHAISSON, M. & GINGERAS, T. R. 2013. STAR: ultrafast universal RNA-seq aligner. *Bioinformatics,* 29**,** 15-21.

EL MARABTI, E. & ABDEL-WAHAB, O. 2021. Therapeutic Modulation of RNA Splicing in Malignant and Non-Malignant Disease. *Trends Mol Med,* 27**,** 643-659.

ELLIS, J. D., BARRIOS-RODILES, M., COLAK, R., IRIMIA, M., KIM, T., CALARCO, J. A., WANG, X., PAN, Q., O'HANLON, D., KIM, P. M., WRANA, J. L. & BLENCOWE, B. J. 2012. Tissue-specific alternative splicing remodels protein-protein interaction networks. *Mol Cell,* 46**,** 884-92.

FELEKE, R., REYNOLDS, R. H., SMITH, A. M., TILLEY, B., TALIUN, S. A. G., HARDY, J., MATTHEWS, P. M., GENTLEMAN, S., OWEN, D. R., JOHNSON, M. R., SRIVASTAVA, P. K. & RYTEN, M. 2021. Cross-platform transcriptional profiling identifies common and distinct molecular pathologies in Lewy body diseases. *Acta Neuropathol,* 142**,** 449-474.

FERNANDES GOMES, B., FARRIS, C. M., MA, Y., CONCHA-MARAMBIO, L., LEBOVITZ, R., NELLGARD, B., DALLA, K., CONSTANTINESCU, J., CONSTANTINESCU, R., GOBOM, J., ANDREASSON, U., ZETTERBERG, H. & BLENNOW, K. 2023. alpha-Synuclein seed amplification assay as a diagnostic tool for parkinsonian disorders. *Parkinsonism Relat Disord,* 117**,** 105807.

FU, R. H., LIU, S. P., HUANG, S. J., CHEN, H. J., CHEN, P. R., LIN, Y. H., HO, Y. C., CHANG, W. L., TSAI, C. H., SHYU, W. C. & LIN, S. Z. 2013. Aberrant alternative splicing events in Parkinson's disease. *Cell Transplant,* 22**,** 653-61.

GEBAUER, F., SCHWARZL, T., VALCARCEL, J. & HENTZE, M. W. 2021. RNA-binding proteins in human genetic disease. *Nat Rev Genet,* 22**,** 185-198.

HUANG, X., KONG, N., ZHANG, X., CAO, Y., LANGER, R. & TAO, W. 2022. The landscape of mRNA nanomedicine. *Nat Med,* 28**,** 2273-2287.

ISAACS, D., CLAASSEN, D., BOWMAN, A. B. & HEDERA, P. 2017. Phenotypic Discordance in Siblings with Identical Compound Heterozygous PARK2 Mutations. *Brain Sci,* 7.

JAGTAP, Y. A., KUMAR, P., KINGER, S., DUBEY, A. R., CHOUDHARY, A., GUTTI, R. K., SINGH, S., JHA, H. C., POLURI, K. M. & MISHRA, A. 2023. Disturb mitochondrial associated proteostasis: Neurodegeneration and imperfect ageing. *Front Cell Dev Biol,* 11**,** 1146564.

JIANG, H., LIU, Y., QIAN, Y., SHEN, Z., HE, Y., GAO, R., SHEN, M., CHEN, S., FU, Q. & YANG, T. 2020. CHL1 promotes insulin secretion and negatively regulates the proliferation of pancreatic beta cells. *Biochem Biophys Res Commun,* 525**,** 1095-1102.

JOSEPH, C., MANGANI, A. S., GUPTA, V., CHITRANSHI, N., SHEN, T., DHEER, Y., KB, D., MIRZAEI, M., YOU, Y., GRAHAM, S. L. & GUPTA, V. 2020. Cell Cycle Deficits in Neurodegenerative Disorders: Uncovering Molecular Mechanisms to Drive Innovative Therapeutic Development. *Aging Dis,* 11**,** 946-966.

KAPELI, K., MARTINEZ, F. J. & YEO, G. W. 2017. Genetic mutations in RNA-binding proteins and their roles in ALS. *Hum Genet,* 136**,** 1193-1214.

KASTNER, B., WILL, C. L., STARK, H. & LUHRMANN, R. 2019. Structural Insights into Nuclear pre-mRNA Splicing in Higher Eukaryotes. *Cold Spring Harb Perspect Biol,* 11.

KIM, T. W., PIAO, J., KOO, S. Y., KRIKS, S., CHUNG, S. Y., BETEL, D., SOCCI, N. D., CHOI, S. J., ZABIEROWSKI, S., DUBOSE, B. N., HILL, E. J., MOSHAROV, E. V., IRION, S., TOMISHIMA, M. J., TABAR, V. & STUDER, L. 2021. Biphasic Activation of WNT Signaling Facilitates the Derivation of Midbrain Dopamine Neurons from hESCs for Translational Use. *Cell Stem Cell,* 28**,** 343-355 e5.

KOULI, A., TORSNEY, K. M. & KUAN, W. L. 2018. Parkinson's Disease: Etiology, Neuropathology, and Pathogenesis. *In:* STOKER, T. B. & GREENLAND, J. C. (eds.) *Parkinson's Disease: Pathogenesis and Clinical Aspects.* Brisbane (AU).

KRUGER, R., KUHN, W., MULLER, T., WOITALLA, D., GRAEBER, M., KOSEL, S., PRZUNTEK, H., EPPLEN, J. T., SCHOLS, L. & RIESS, O. 1998. Ala30Pro mutation in the gene encoding alpha-synuclein in Parkinson's disease. *Nat Genet,* 18**,** 106-8.

KWON, D. K., KWATRA, M., WANG, J. & KO, H. S. 2022. Levodopa-Induced Dyskinesia in Parkinson's Disease: Pathogenesis and Emerging Treatment Strategies. *Cells,* 11.

LEE, Y. J., WANG, Q. Q. & RIO, D. C. 2018. Coordinate regulation of alternative pre-mRNA splicing events by the human RNA chaperone proteins hnRNPA1 and DDX5. *Genes & Development,* 32**,** 1060-1074.

LEHTONEN, S., SONNINEN, T. M., WOJCIECHOWSKI, S., GOLDSTEINS, G. & KOISTINAHO, J. 2019. Dysfunction of Cellular Proteostasis in Parkinson's Disease. *Front Neurosci,* 13**,** 457.

LI, D., MASTAGLIA, F. L., YAU, W. Y., CHEN, S., WILTON, S. D. & AKKARI, P. A. 2022a. Targeted Molecular Therapeutics for Parkinson's Disease: A Role for Antisense Oligonucleotides? *Mov Disord,* 37**,** 2184-2190.

LI, D., MCINTOSH, C. S., MASTAGLIA, F. L., WILTON, S. D. & AUNG-HTUT, M. T. 2021. Neurodegenerative diseases: a hotbed for splicing defects and the potential therapies. *Transl Neurodegener,* 10**,** 16.

LI, H., BUSQUETS, O., VERMA, Y., SYED, K. M., KUTNOWSKI, N., PANGILINAN, G. R., GILBERT, L. A., BATEUP, H. S., RIO, D. C., HOCKEMEYER, D. & SOLDNER, F. 2022b. Highly efficient generation of isogenic pluripotent stem cell models using prime editing. *Elife,* 11.

LI, Y., ZENG, H., WEI, Y., MA, X. & HE, Z. 2023. An Overview of the Therapeutic Strategies for the Treatment of Spinal Muscular Atrophy. *Hum Gene Ther,* 34**,** 180-191.

LI, Y. I., KNOWLES, D. A., HUMPHREY, J., BARBEIRA, A. N., DICKINSON, S. P., IM, H. K. & PRITCHARD, J. K. 2018. Annotation-free quantification of RNA splicing using LeafCutter. *Nat Genet,* 50**,** 151-158.

LIPSTEIN, N. 2022. Mechanism underlying a risk gene in neurodegeneration. *Nature,* 603**,** 33-34.

LOVE, M. I., HUBER, W. & ANDERS, S. 2014. Moderated estimation of fold change and dispersion for RNA-seq data with DESeq2. *Genome Biol,* 15**,** 550.

MA, X. R., PRUDENCIO, M., KOIKE, Y., VATSAVAYAI, S. C., KIM, G., HARBINSKI, F., BRINER, A., RODRIGUEZ, C. M., GUO, C., AKIYAMA, T., SCHMIDT, H. B., CUMMINGS, B. B., WYATT, D. W., KURYLO, K., MILLER, G., MEKHOUBAD, S., SALLEE, N., MEKONNEN, G., GANSER, L., RUBIEN, J. D., JANSEN-WEST, K., COOK, C. N., PICKLES, S., OSKARSSON, B., GRAFF-RADFORD, N. R., BOEVE, B. F., KNOPMAN, D. S., PETERSEN, R. C., DICKSON, D. W., SHORTER, J., MYONG, S., GREEN, E. M., SEELEY, W. W., PETRUCELLI, L. & GITLER, A. D. 2022. TDP-43 represses cryptic exon inclusion in the FTD-ALS gene UNC13A. *Nature,* 603**,** 124-130.

MANN, J. R. & DONNELLY, C. J. 2021. RNA modulates physiological and neuropathological protein phase transitions. *Neuron,* 109**,** 2663-2681.

MEHTA, P. R., BROWN, A. L., WARD, M. E. & FRATTA, P. 2023. The era of cryptic exons: implications for ALS-FTD. *Mol Neurodegener,* 18**,** 16.

MENDOZA-VELASQUEZ, J. J., FLORES-VAZQUEZ, J. F., BARRON-VELAZQUEZ, E., SOSA-ORTIZ, A. L., ILLIGENS, B. W. & SIEPMANN, T. 2019. Autonomic Dysfunction in alpha-Synucleinopathies. *Front Neurol,* 10**,** 363.

MEYER, S. M., WILLIAMS, C. C., AKAHORI, Y., TANAKA, T., AIKAWA, H., TONG, Y., CHILDS-DISNEY, J. L. & DISNEY, M. D. 2020. Small molecule recognition of disease-relevant RNA structures. *Chem Soc Rev,* 49**,** 7167-7199.

MOHAN, V., WADE, S. D., SULLIVAN, C. S., KASTEN, M. R., SWEETMAN, C., STEWART, R., TRUONG, Y., SCHACHNER, M., MANIS, P. B. & MANESS, P. F. 2019. Close Homolog of L1 Regulates Dendritic Spine Density in the Mouse Cerebral Cortex Through Semaphorin 3B. *J Neurosci,* 39**,** 6233-6250.

NAVARRO-ROMERO, A., MONTPEYO, M. & MARTINEZ-VICENTE, M. 2020. The Emerging Role of the Lysosome in Parkinson's Disease. *Cells,* 9.

NIKOM, D. & ZHENG, S. 2023. Alternative splicing in neurodegenerative disease and the promise of RNA therapies. *Nat Rev Neurosci,* 24**,** 457-473.

NITURAD, C. E., LEV, D., KALSCHEUER, V. M., CHARZEWSKA, A., SCHUBERT, J., LERMAN-SAGIE, T., KROES, H. Y., OEGEMA, R., TRAVERSO, M., SPECCHIO, N., LASSOTA, M., CHELLY, J., BENNETT-BACK, O., CARMI, N., KOFFLER-BRILL, T., IACOMINO, M., TRIVISANO, M., CAPOVILLA, G., STRIANO, P., NAWARA, M., RZONCA, S., FISCHER, U., BIENEK, M., JENSEN, C., HU, H., THIELE, H., ALTMULLER, J., KRAUSE, R., MAY, P., BECKER, F., EURO, E. C., BALLING, R., BISKUP, S., HAAS, S. A., NURNBERG, P., VAN GASSEN, K. L. I., LERCHE, H., ZARA, F., MALJEVIC, S. & LESHINSKY-SILVER, E. 2017. Rare GABRA3 variants are associated with epileptic seizures, encephalopathy and dysmorphic features. *Brain,* 140**,** 2879-2894.

NUSSBACHER, J. K., TABET, R., YEO, G. W. & LAGIER-TOURENNE, C. 2019. Disruption of RNA Metabolism in Neurological Diseases and Emerging Therapeutic Interventions. *Neuron,* 102**,** 294-320.

O'HARA, D. M., PAWAR, G., KALIA, S. K. & KALIA, L. V. 2020. LRRK2 and alpha-Synuclein: Distinct or Synergistic Players in Parkinson's Disease? *Front Neurosci,* 14**,** 577.

PFEFFER, S. R. 2018. LRRK2 and Rab GTPases. *Biochem Soc Trans,* 46**,** 1707-1712.

PFEFFER, S. R. 2023. LRRK2 phosphorylation of Rab GTPases in Parkinson's disease. *FEBS Lett,* 597**,** 811-818.

PLACEK, K., BAER, G. M., ELMAN, L., MCCLUSKEY, L., HENNESSY, L., FERRARO, P. M., LEE, E. B., LEE, V. M. Y., TROJANOWSKI, J. Q., VAN DEERLIN, V. M., GROSSMAN, M., IRWIN, D. J. & MCMILLAN, C. T. 2019. UNC13A polymorphism contributes to frontotemporal disease in sporadic amyotrophic lateral sclerosis. *Neurobiol Aging,* 73**,** 190-199.

PLASCHKA, C., NEWMAN, A. J. & NAGAI, K. 2019. Structural Basis of Nuclear pre-mRNA Splicing: Lessons from Yeast. *Cold Spring Harb Perspect Biol,* 11.

PLOTEGHER, N. & DUCHEN, M. R. 2017. Crosstalk between Lysosomes and Mitochondria in Parkinson's Disease. *Front Cell Dev Biol,* 5**,** 110.

POEWE, W., SEPPI, K., TANNER, C. M., HALLIDAY, G. M., BRUNDIN, P., VOLKMANN, J., SCHRAG, A. E. & LANG, A. E. 2017. Parkinson disease. *Nat Rev Dis Primers,* 3**,** 17013.

POLYMEROPOULOS, M. H., LAVEDAN, C., LEROY, E., IDE, S. E., DEHEJIA, A., DUTRA, A., PIKE, B., ROOT, H., RUBENSTEIN, J., BOYER, R., STENROOS, E. S., CHANDRASEKHARAPPA, S., ATHANASSIADOU, A., PAPAPETROPOULOS, T., JOHNSON, W. G., LAZZARINI, A. M., DUVOISIN, R. C., DI IORIO, G., GOLBE, L. I. & NUSSBAUM, R. L. 1997. Mutation in the alpha-synuclein gene identified in families with Parkinson's disease. *Science,* 276**,** 2045-7.

POTASHKIN, J. A., SANTIAGO, J. A., RAVINA, B. M., WATTS, A. & LEONTOVICH, A. A. 2012. Biosignatures for Parkinson's disease and atypical parkinsonian disorders patients. *PLoS One,* 7**,** e43595.

PU, J. L., GAO, T., SI, X. L., ZHENG, R., JIN, C. Y., RUAN, Y., FANG, Y., CHEN, Y., SONG, Z., YIN, X. Z., YAN, Y. P., TIAN, J. & ZHANG, B. R. 2020. Parkinson's Disease in Teneurin Transmembrane Protein 4 (TENM4) Mutation Carriers. *Front Genet,* 11**,** 598064.

REGAN-FENDT, K. E., RIPPERT, A. L., MEDNE, L., SKRABAN, C. M., DEJESSE, J., GRAY, C., REICHERT, S. L., STAROPOLI, N. P., SANTOS, F. J. R., KRANTZ, I. D., MURRELL, J. R. & IZUMI, K. 2023. Retrospective identification of patients with SRRM2-related neurodevelopmental disorder in a single tertiary children's hospital. *Am J Med Genet A,* 191**,** 2149-2155.

ROGALSKA, M. E., VIVORI, C. & VALCARCEL, J. 2023. Regulation of pre-mRNA splicing: roles in physiology and disease, and therapeutic prospects. *Nat Rev Genet,* 24**,** 251-269.

SANTIAGO, J. A., SCHERZER, C. R., HARVARD BIOMARKER, S. & POTASHKIN, J. A. 2013. Specific splice variants are associated with Parkinson's disease. *Mov Disord,* 28**,** 1724-7.

SASAKI, S., SHIRATA, A., YAMANE, K. & IWATA, M. 2004. Parkin-positive autosomal recessive juvenile Parkinsonism with alpha-synuclein-positive inclusions. *Neurology,* 63**,** 678-82.

SCHEKMAN, R. & RILEY, E. A. U. 2019. Coordinating a new approach to basic research into Parkinson's disease. *eLife,* 8**,** e51167.

SHEHADEH, L. A., YU, K., WANG, L., GUEVARA, A., SINGER, C., VANCE, J. & PAPAPETROPOULOS, S. 2010. SRRM2, a potential blood biomarker revealing high alternative splicing in Parkinson's disease. *PLoS One,* 5**,** e9104.

SHI, X., ZHENG, J., MA, J., WANG, Z., SUN, W., LI, M., HUANG, S. & HU, S. 2022. Insulin-like growth factor in Parkinson's disease is related to nonmotor symptoms and the volume of specific brain areas. *Neurosci Lett,* 783**,** 136735.

SHINODA, Y., SADAKATA, T., NAKAO, K., KATOH-SEMBA, R., KINAMERI, E., FURUYA, A., YANAGAWA, Y., HIRASE, H. & FURUICHI, T. 2011. Calcium-dependent activator protein for secretion 2 (CAPS2) promotes BDNF secretion and is critical for the development of GABAergic interneuron network. *Proc Natl Acad Sci U S A,* 108**,** 373-8.

SINGH, R. N. & SINGH, N. N. 2018. Mechanism of Splicing Regulation of Spinal Muscular Atrophy Genes. *Adv Neurobiol,* 20**,** 31-61.

SOREQ, L., BERGMAN, H., ISRAEL, Z. & SOREQ, H. 2012. Exon arrays reveal alternative splicing aberrations in Parkinson's disease leukocytes. *Neurodegener Dis,* 10**,** 203-6.

STANLEY, R. F. & ABDEL-WAHAB, O. 2022. Dysregulation and therapeutic targeting of RNA splicing in cancer. *Nat Cancer,* 3**,** 536-546.

SU, C. H., D, D. & TARN, W. Y. 2018. Alternative Splicing in Neurogenesis and Brain Development. *Front Mol Biosci,* 5**,** 12.

TRAPNELL, C., PACHTER, L. & SALZBERG, S. L. 2009. TopHat: discovering splice junctions with RNA-Seq. *Bioinformatics,* 25**,** 1105-11.

WANG, Q., CONLON, E. G., MANLEY, J. L. & RIO, D. C. 2020. Widespread intron retention impairs protein homeostasis in C9orf72 ALS brains. *Genome Res,* 30**,** 1705-1715.

WANG, Q. & RIO, D. C. 2018. JUM is a computational method for comprehensive annotation-free analysis of alternative pre-mRNA splicing patterns. *Proceedings of the National Academy of Sciences of the United States of America,* 115**,** E8181-E8190.

WILL, C. L. & LUHRMANN, R. 2011. Spliceosome structure and function. *Cold Spring Harb Perspect Biol,* 3.

WILLEMSE, S. W., HARLEY, P., VAN EIJK, R. P. A., DEMAEGD, K. C., ZELINA, P., PASTERKAMP, R. J., VAN DAMME, P., INGRE, C., VAN RHEENEN, W., VELDINK, J. H., KIERNAN, M. C., AL-CHALABI, A., VAN DEN BERG, L. H., FRATTA, P. & VAN ES, M. A. 2023. UNC13A in amyotrophic lateral sclerosis: from genetic association to therapeutic target. *J Neurol Neurosurg Psychiatry,* 94**,** 649-656.

WILSON, D. M., 3RD, COOKSON, M. R., VAN DEN BOSCH, L., ZETTERBERG, H., HOLTZMAN, D. M. & DEWACHTER, I. 2023. Hallmarks of neurodegenerative diseases. *Cell,* 186**,** 693-714.

WINSLOW, A. R., CHEN, C. W., CORROCHANO, S., ACEVEDO-AROZENA, A., GORDON, D. E., PEDEN, A. A., LICHTENBERG, M., MENZIES, F. M., RAVIKUMAR, B., IMARISIO, S., BROWN, S., O'KANE, C. J. & RUBINSZTEIN, D. C. 2010. alpha-Synuclein impairs macroautophagy: implications for Parkinson's disease. *J Cell Biol,* 190**,** 1023-37.

YAO, J., GAO, R., LUO, M., LI, D., GUO, L., YU, Z., XIONG, F., WEI, C., WU, B., XU, Z., ZHANG, D., WANG, J. & WANG, L. 2020. Close homolog of L1-deficient ameliorates inflammatory bowel disease by regulating the balance of Th17/Treg. *Gene,* 757**,** 144931.

ZHANG, J. & MANLEY, J. L. 2013. Misregulation of pre-mRNA alternative splicing in cancer. *Cancer Discov,* 3**,** 1228-37.

Authors' ORCID ID:

Yeon Lee http://orcid.org/0000-0003-3756-4515

Khaja Mohieddin Syed http://orcid.org/0000-0002-7682-7608

Hanqin Li http://orcid.org/0000-0001-7995-1084

Oriol Busquets http://orcid.org/0000-0002-1372-9699

Jesse Dunnack http://orcid.org/0000-0002-0387-0090

Atehsa Sahagun http://orcid.org/0000-0001-7521-3279

Helen S Bateup http://orcid.org/0000-0002-0135-0972

Dirk Hockemeyer http://orcid.org/0000-0002-5598-5092

Frank Soldner http://orcid.org/0000-0002-7102-8655

Donald C Rio http://orcid.org/0000-0002-4775-3515

Figure 1

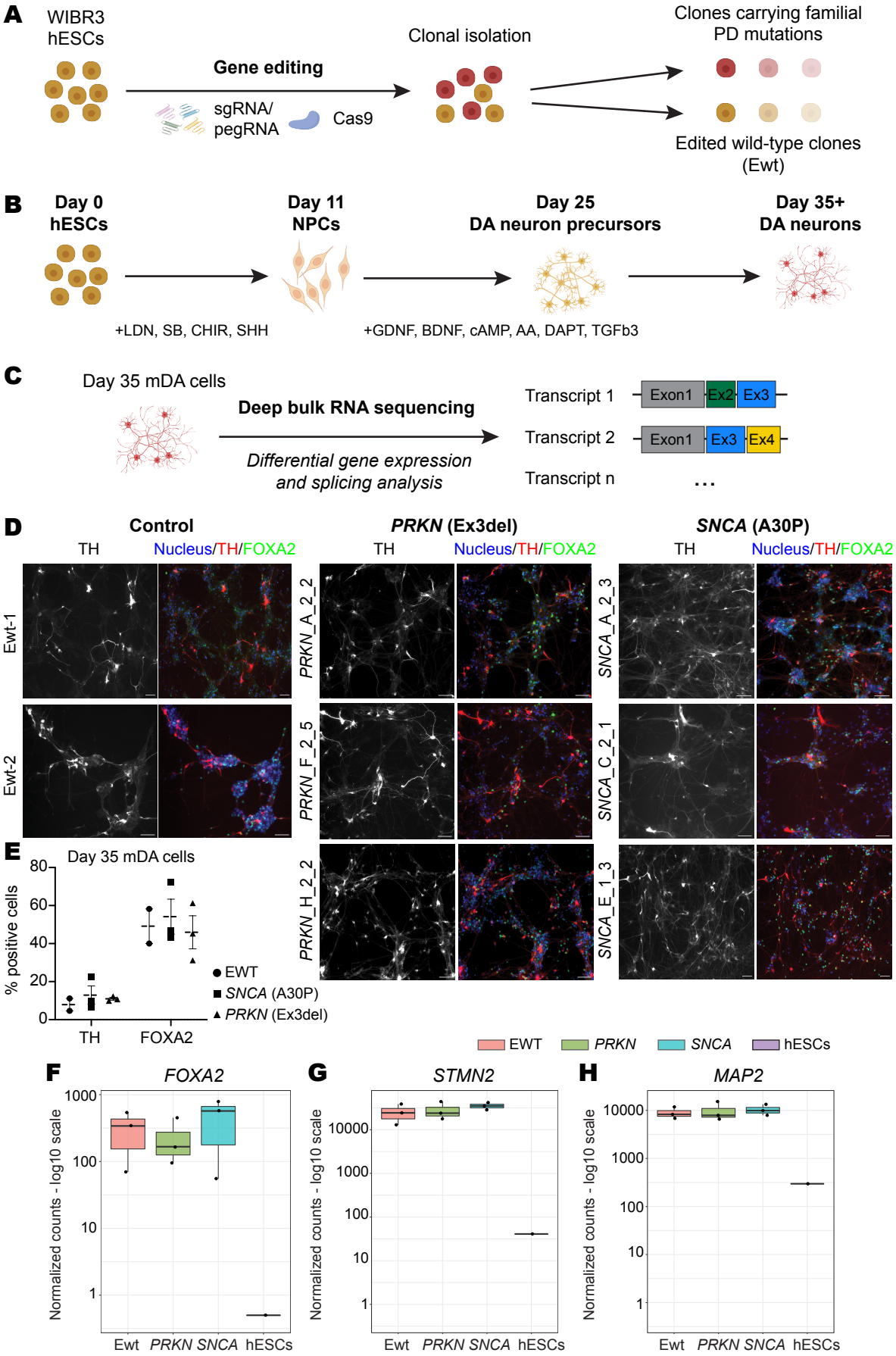
A
WIBR3 hESCs
Gene editing
sgRNA/ pegRNA
Cas9
Clonal isolation
Clones carrying familial PD mutations
Edited wild-type clones (Ewt)
B
Day 0 hESCs
Day 11 NPCs
Day 25 DA neuron precursors
Day 35+ DA neurons
+LDN, SB, CHIR, SHH
+GDNF, BDNF, cAMP, AA, DAPT, TGFb3
C
Day 35 mDA cells
Deep bulk RNA sequencing
Differential gene expression and splicing analysis
Transcript 1
Exon1
Ex2
Ex3
Transcript 2
Exon1
Ex3
Ex4
Transcript n
...
D
Control
PRKN (Ex3del)
SNCA (A30P)
TH
Nucleus/TH/FOXA2
Ewt-1
Ewt-2
PRKN_A_2_2
PRKN_F_2_5
PRKN_H_2_2
SNCA_A_2_3
SNCA_C_2_1
SNCA_E_1_3
E
Day 35 mDA cells
% positive cells
80
60
40
20
0
TH
FOXA2
EWT
SNCA (A30P)
PRKN (Ex3del)
EWT
PRKN
SNCA
hESCs
F
FOXA2
G
STMN2
H
MAP2
Normalized counts - log10 scale
1000
100
10
1
10000
Ewt
PRKN
SNCA
hESCs

Figure 2.

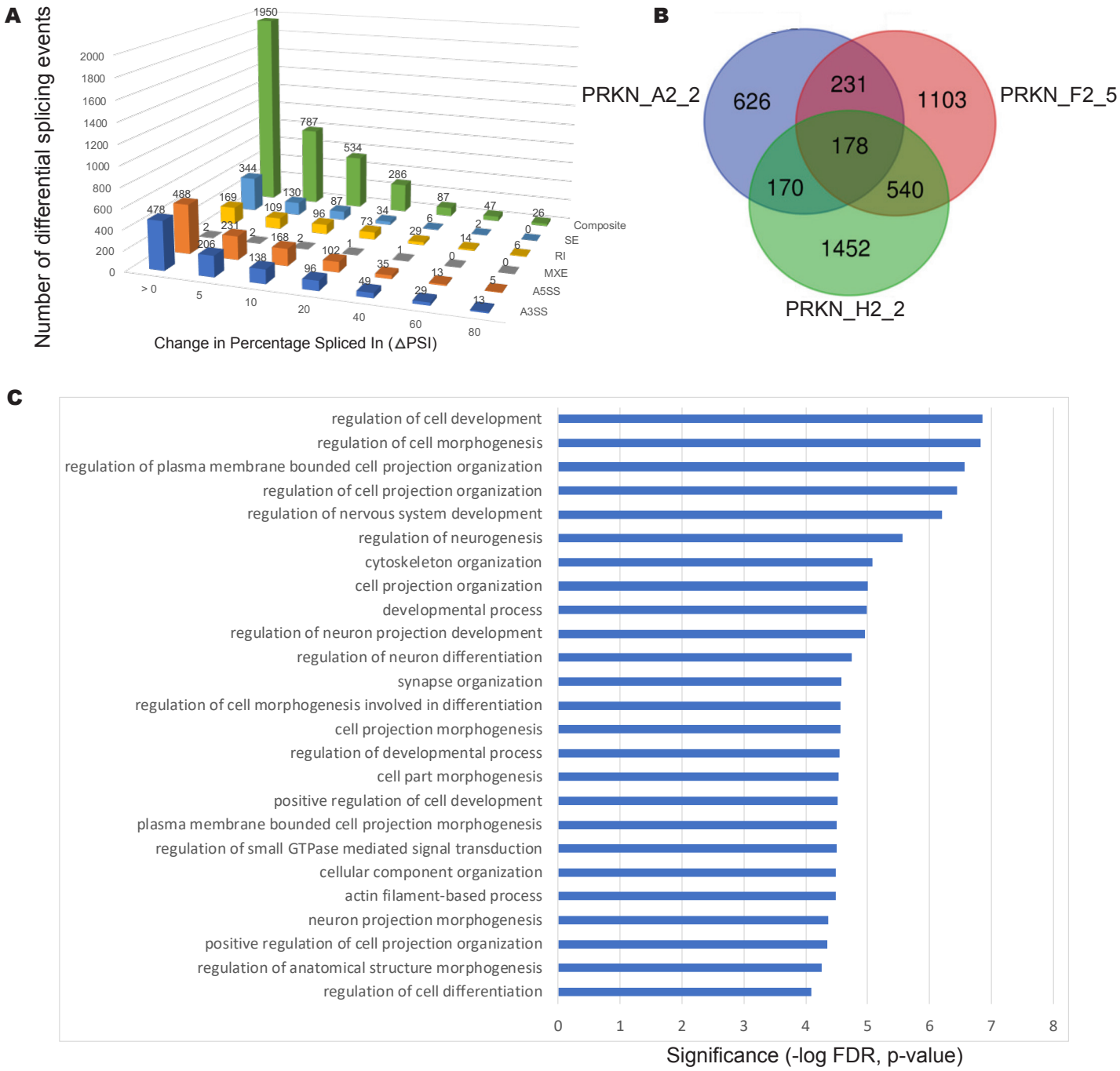
A
Number of differential splicing events
Change in Percentage Spliced In (ΔPSI)
Composite
SE
RI
MXE
A5SS
A3SS
B
PRKN_A2_2
PRKN_F2_5
PRKN_H2_2
626
231
1103
178
170
540
1452
C
regulation of cell development
regulation of cell morphogenesis
regulation of plasma membrane bounded cell projection organization
regulation of cell projection organization
regulation of nervous system development
regulation of neurogenesis
cytoskeleton organization
cell projection organization
developmental process
regulation of neuron projection development
regulation of neuron differentiation
synapse organization
regulation of cell morphogenesis involved in differentiation
cell projection morphogenesis
regulation of developmental process
cell part morphogenesis
positive regulation of cell development
plasma membrane bounded cell projection morphogenesis
regulation of small GTPase mediated signal transduction
cellular component organization
actin filament-based process
neuron projection morphogenesis
positive regulation of cell projection organization
regulation of anatomical structure morphogenesis
regulation of cell differentiation
Significance (-log FDR, p-value)

Figure 3.

A

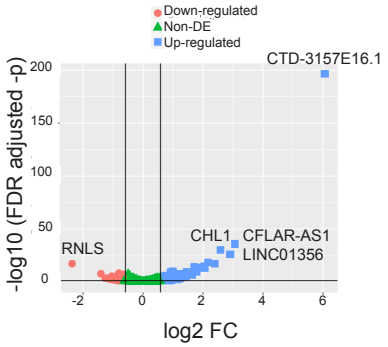
Down-regulated
Non-DE
Up-regulated
CTD-3157E16.1
RNLS
CHL1
CFLAR-AS1
LINC01356
-log10 (FDR adjusted -p)
log2 FC

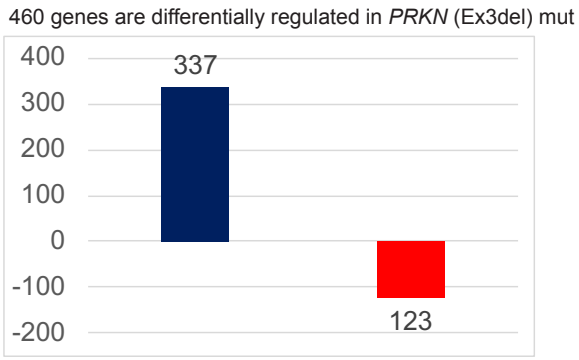
460 genes are differentially regulated in PRKN (Ex3del) mut
337
123

B

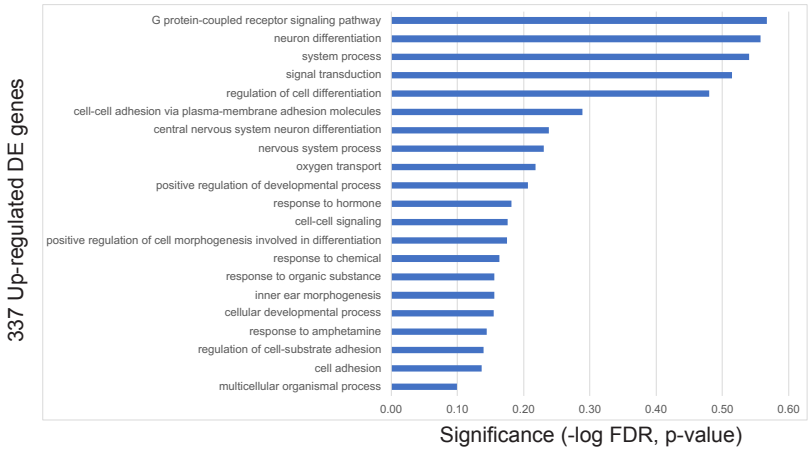
337 Up-regulated DE genes
G protein-coupled receptor signaling pathway
neuron differentiation
system process
signal transduction
regulation of cell differentiation
cell-cell adhesion via plasma-membrane adhesion molecules
central nervous system neuron differentiation
nervous system process
oxygen transport
positive regulation of developmental process
response to hormone
cell-cell signaling
positive regulation of cell morphogenesis involved in differentiation
response to chemical
response to organic substance
inner ear morphogenesis
cellular developmental process
response to amphetamine
regulation of cell-substrate adhesion
cell adhesion
multicellular organismal process
Significance (-log FDR, p-value)

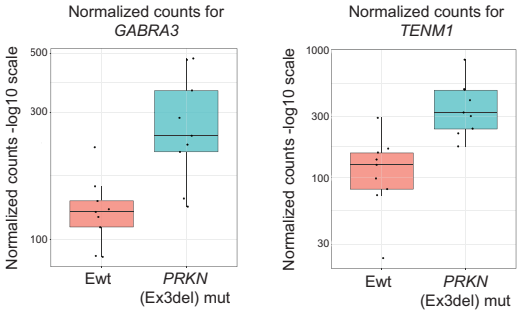
Normalized counts for GABRA3
Normalized counts for TENM1
Normalized counts -log10 scale
Ewt
PRKN (Ex3del) mut

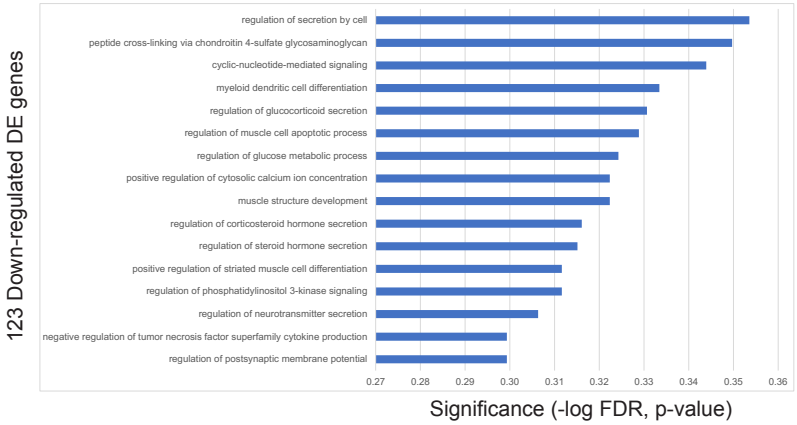
123 Down-regulated DE genes
regulation of secretion by cell
peptide cross-linking via chondroitin 4-sulfate glycosaminoglycan
cyclic-nucleotide-mediated signaling
myeloid dendritic cell differentiation
regulation of glucocorticoid secretion
regulation of muscle cell apoptotic process
regulation of glucose metabolic process
positive regulation of cytosolic calcium ion concentration
muscle structure development
regulation of corticosteroid hormone secretion
regulation of steroid hormone secretion
positive regulation of striated muscle cell differentiation
regulation of phosphatidylinositol 3-kinase signaling
regulation of neurotransmitter secretion
negative regulation of tumor necrosis factor superfamily cytokine production
regulation of postsynaptic membrane potential
Significance (-log FDR, p-value)

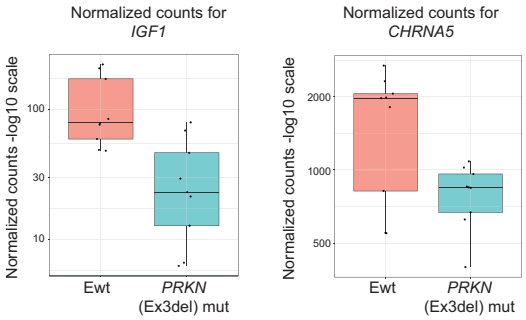
Normalized counts for IGF1
Normalized counts for CHRNA5
Normalized counts -log10 scale
Ewt
PRKN (Ex3del) mut

C

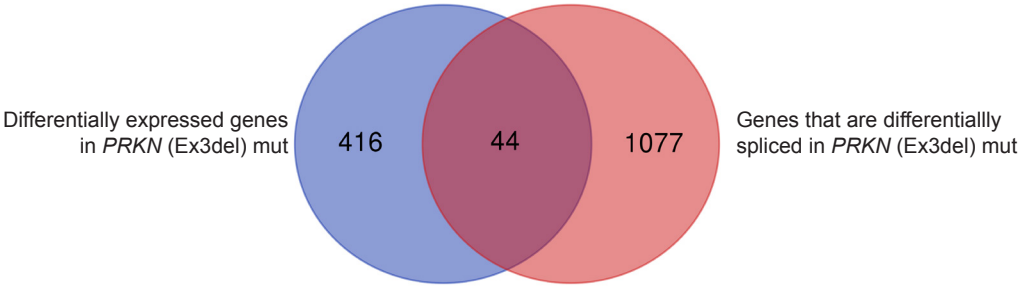
Differentially expressed genes in PRKN (Ex3del) mut
416
44
1077
Genes that are differentiallly spliced in PRKN (Ex3del) mut

Figure 4.

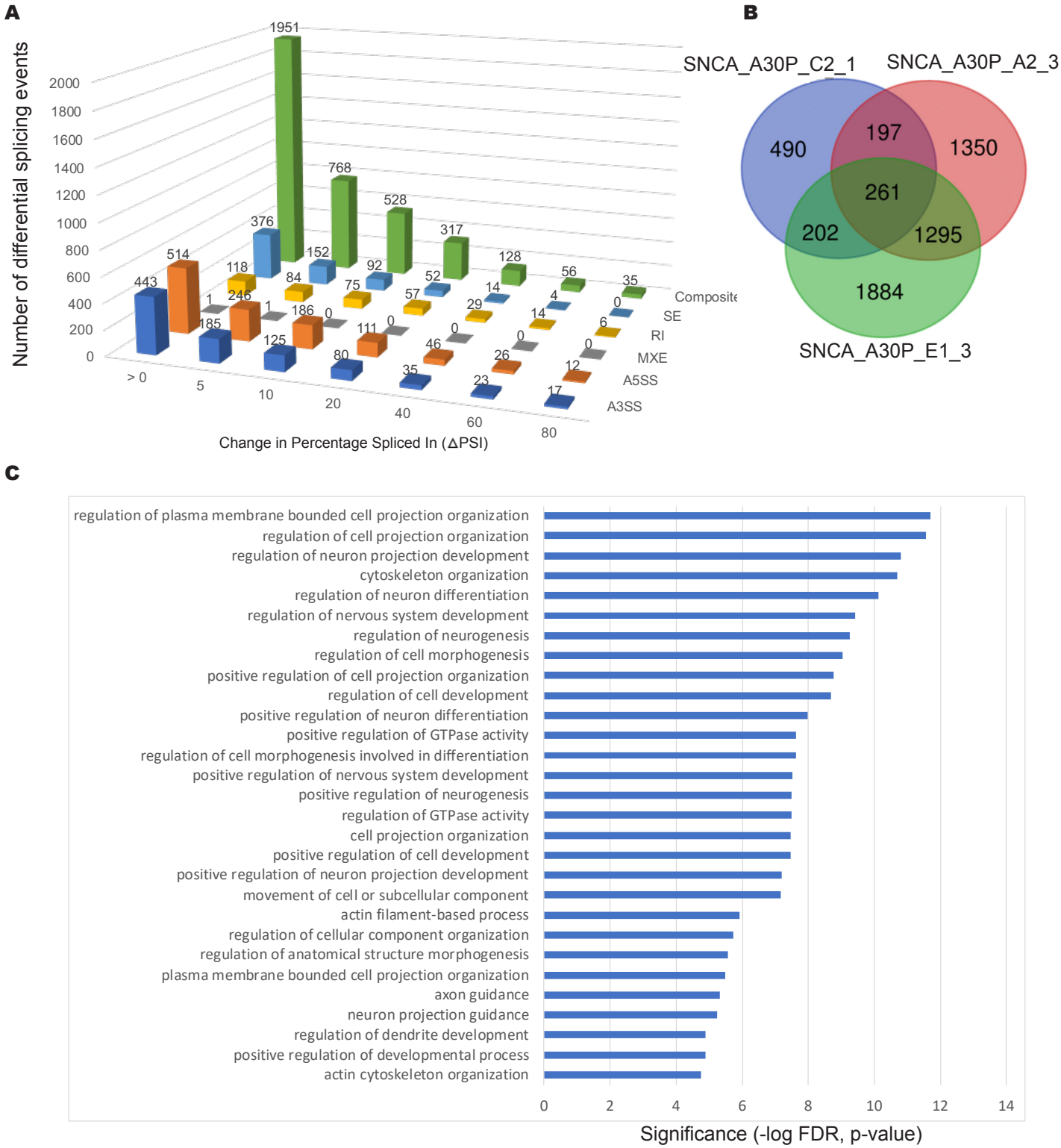
A
Number of differential splicing events
2000
1800
1600
1400
1200
1000
800
600
400
200
0
1951
768
528
317
376
152
128
514
118
92
56
443
84
75
52
35
1
246
1
57
14
4
0
185
186
0
29
14
6
125
111
0
0
0
80
46
26
12
35
23
17
> 0
5
10
20
40
60
80
Composite
SE
RI
MXE
A5SS
A3SS
Change in Percentage Spliced In (ΔPSI)
B
SNCA_A30P_C2_1
SNCA_A30P_A2_3
SNCA_A30P_E1_3
490
197
1350
261
202
1295
1884
C
regulation of plasma membrane bounded cell projection organization
regulation of cell projection organization
regulation of neuron projection development
cytoskeleton organization
regulation of neuron differentiation
regulation of nervous system development
regulation of neurogenesis
regulation of cell morphogenesis
positive regulation of cell projection organization
regulation of cell development
positive regulation of neuron differentiation
positive regulation of GTPase activity
regulation of cell morphogenesis involved in differentiation
positive regulation of nervous system development
positive regulation of neurogenesis
regulation of GTPase activity
cell projection organization
positive regulation of cell development
positive regulation of neuron projection development
movement of cell or subcellular component
actin filament-based process
regulation of cellular component organization
regulation of anatomical structure morphogenesis
plasma membrane bounded cell projection organization
axon guidance
neuron projection guidance
regulation of dendrite development
positive regulation of developmental process
actin cytoskeleton organization
0
2
4
6
8
10
12
14
Significance (-log FDR, p-value)

Figure 5.

A

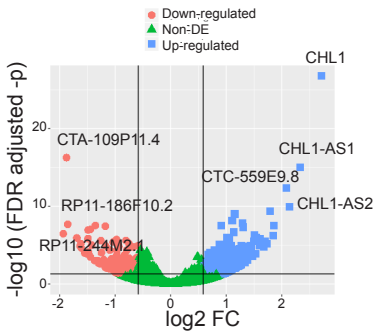
Down-regulated
Non-DE
Up-regulated
CHL1
CTA-109P11.4
CHL1-AS1
CTC-559E9.8
RP11-186F10.2
CHL1-AS2
RP11-244M2.1
-log10 (FDR adjusted -p)
log2 FC

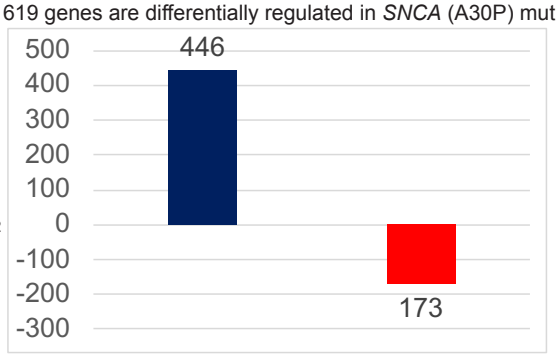
619 genes are differentially regulated in SNCA (A30P) mut
446
173

B

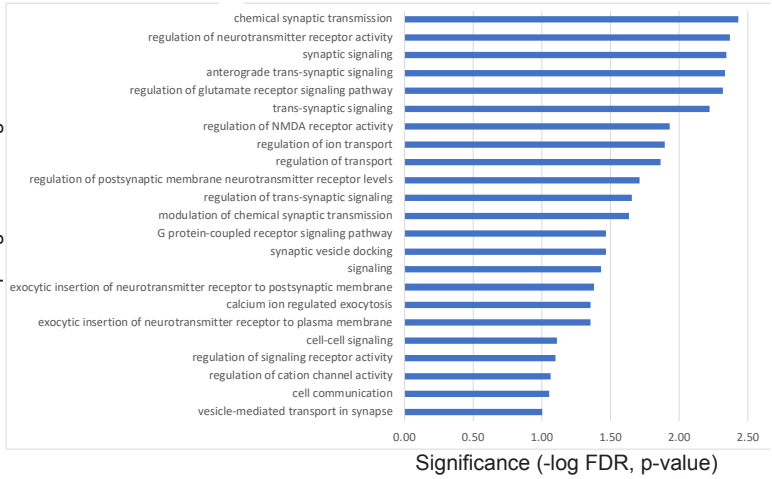
446 Up-regulated DE genes
chemical synaptic transmission
regulation of neurotransmitter receptor activity
synaptic signaling
anterograde trans-synaptic signaling
regulation of glutamate receptor signaling pathway
trans-synaptic signaling
regulation of NMDA receptor activity
regulation of ion transport
regulation of transport
regulation of postsynaptic membrane neurotransmitter receptor levels
regulation of trans-synaptic signaling
modulation of chemical synaptic transmission
G protein-coupled receptor signaling pathway
synaptic vesicle docking
signaling
exocytic insertion of neurotransmitter receptor to postsynaptic membrane
calcium ion regulated exocytosis
exocytic insertion of neurotransmitter receptor to plasma membrane
cell-cell signaling
regulation of signaling receptor activity
regulation of cation channel activity
cell communication
vesicle-mediated transport in synapse
Significance (-log FDR, p-value)

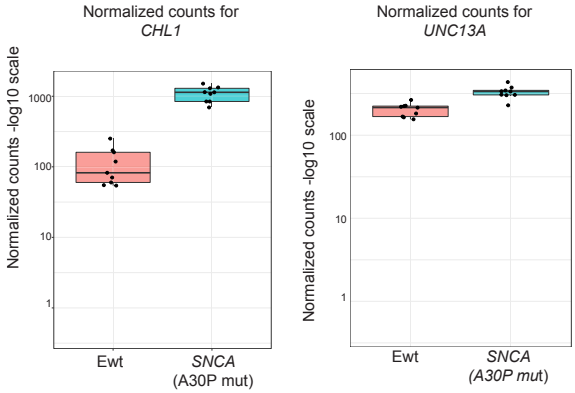
Normalized counts for CHL1
Normalized counts for UNC13A
Normalized counts -log10 scale
Ewt
SNCA (A30P mut)

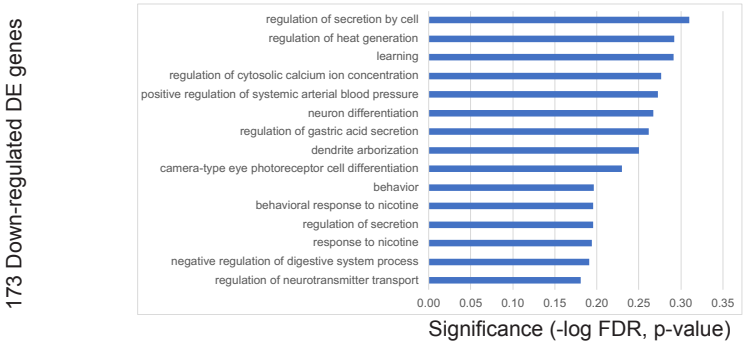
173 Down-regulated DE genes
regulation of secretion by cell
regulation of heat generation
learning
regulation of cytosolic calcium ion concentration
positive regulation of systemic arterial blood pressure
neuron differentiation
regulation of gastric acid secretion
dendrite arborization
camera-type eye photoreceptor cell differentiation
behavior
behavioral response to nicotine
regulation of secretion
response to nicotine
negative regulation of digestive system process
regulation of neurotransmitter transport
Significance (-log FDR, p-value)

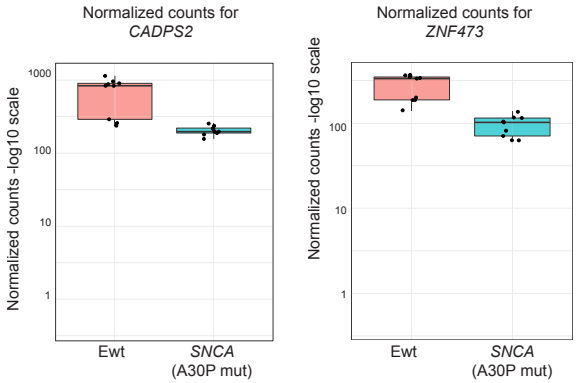
Normalized counts for CADPS2
Normalized counts for ZNF473
Normalized counts -log10 scale
Ewt
SNCA (A30P mut)

C

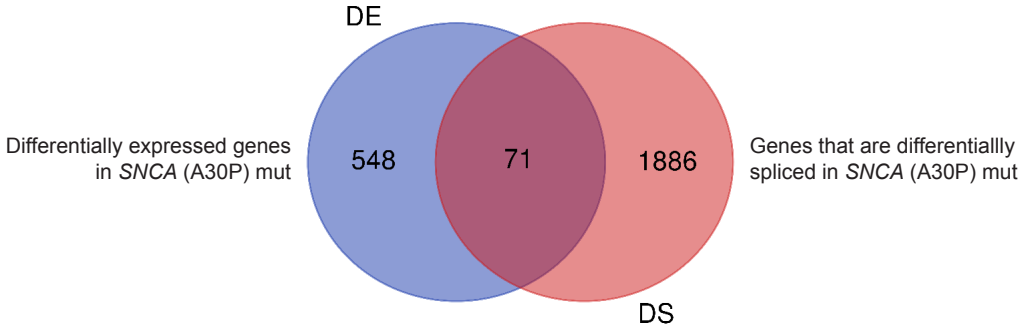
DE
Differentially expressed genes in SNCA (A30P) mut
548
71
1886
Genes that are differentiallly spliced in SNCA (A30P) mut
DS

Figure 6.

A

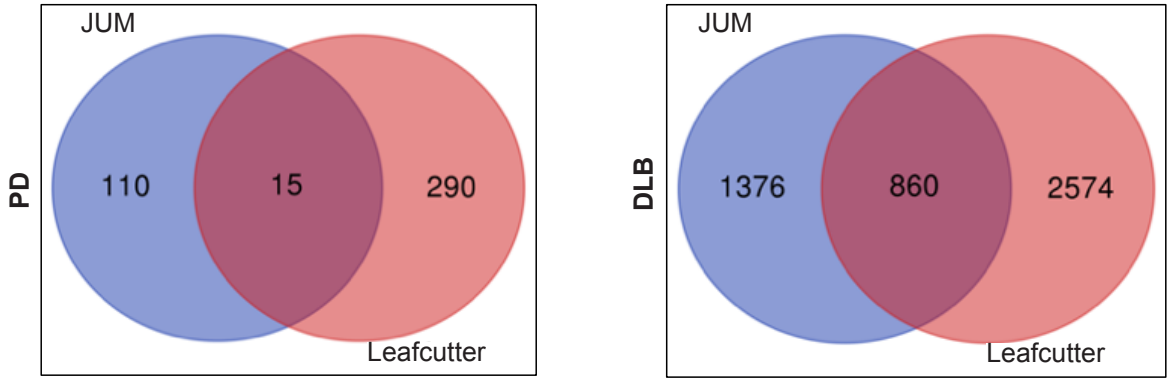

	JUM	Leafcutter
PD	125	305
PDD	168	357
DLB	2,236	3,434

B

PRKN (Exo3del)

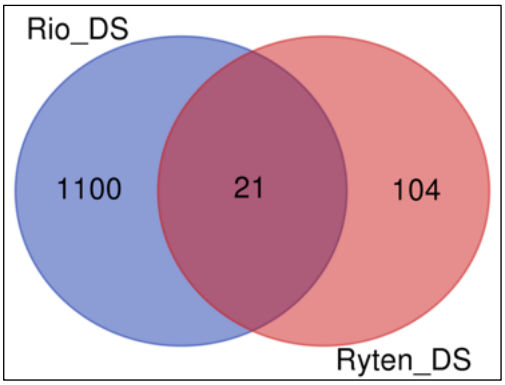

21 common genes:
MACF1, RBFOX1, FYN, CADPS, MAST4, DDX46, ABLIM2, KIDINS220, EPB41L2, DOCK10, EML4, MICAL2, IPO11, ZNF789, CALD1, LINC00403, SRRM2, EVL, NRXN2, PSD3, L3MBTL1

SNCA (A30P)

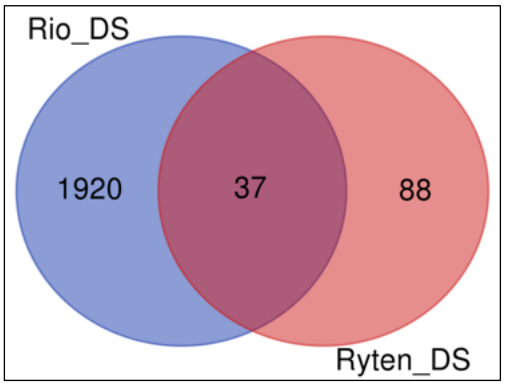

37 common genes:
MACF1, TENM4, ZCWPW1, SEC14L1, UPF3A, EML2, MEF2BNB-MEF2B, FHL1, FYN, CADPS, SYT7, CD46, PRUNE2, TXNL4A, MAST4, AK2, ABLIM2, FMNL1, KIDINS220, EPB41L2, PTPRF, DOCK10, EML4, MICAL2, WDR27, ZNF708, PPP1R21, CALD1, SLIT2, RASGRF2, LINC00403, SRRM2, UBR4, NRXN2, PSD3, L3MBTL1, EVL

Figure 7.

A

DDX46

Region A
Differentially spliced in PD and DLB patients

Region B
Differentially spliced in *PRKN* (Ex3del) mut mDA cells

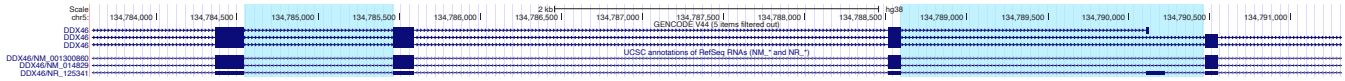

PD patient: JUM - SE
DLB patient data: Leafcutter

PRKN (Ex3del) mut: JUM – composite

SRRM2

Region A
Differentially spliced in PD patients, *PRKN* (Ex3del) mut mDA

Region B
Differentially spliced in Rio ASAP *SNCA (A30P)* mut in mDA cells

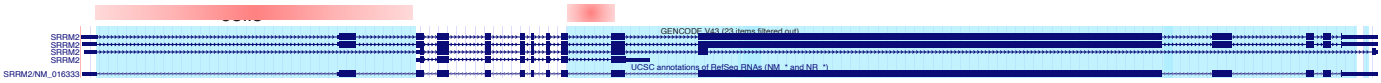

chr16:2752846-2757470 (Ryten PD, A5SS, PSI = -0.06)

Differentially spliced in Rio ASAP *SNCA (A30P)* mut in mDA cells

chr16:2752756-2752825 (PRKN_F2_5,RI, PSI=0.30)
chr16:2759661-2769026 (PRKN_H2_2, composite)
chr16:2759661-2760299 (PRKN_F2_5, composite)

chr16:2759661-2760299 (SNCA_A30P_A2_3, composite)
chr16:2759661-2760299 (SNCA_A30P_E1_3, composite)

chr16:2766398-2766583 (SNCA_A30P_A2_3, A3SS, PSI=-0.14)

B

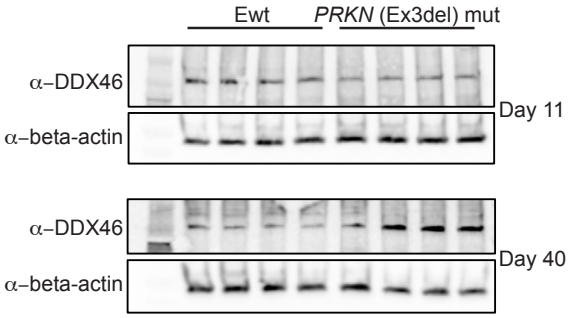

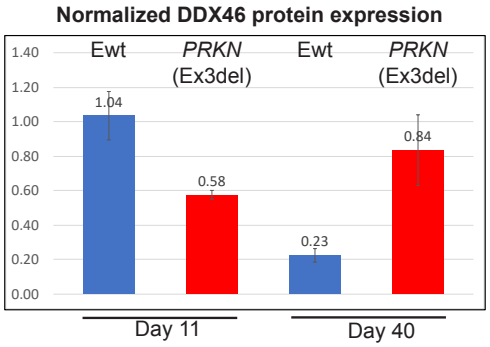

C

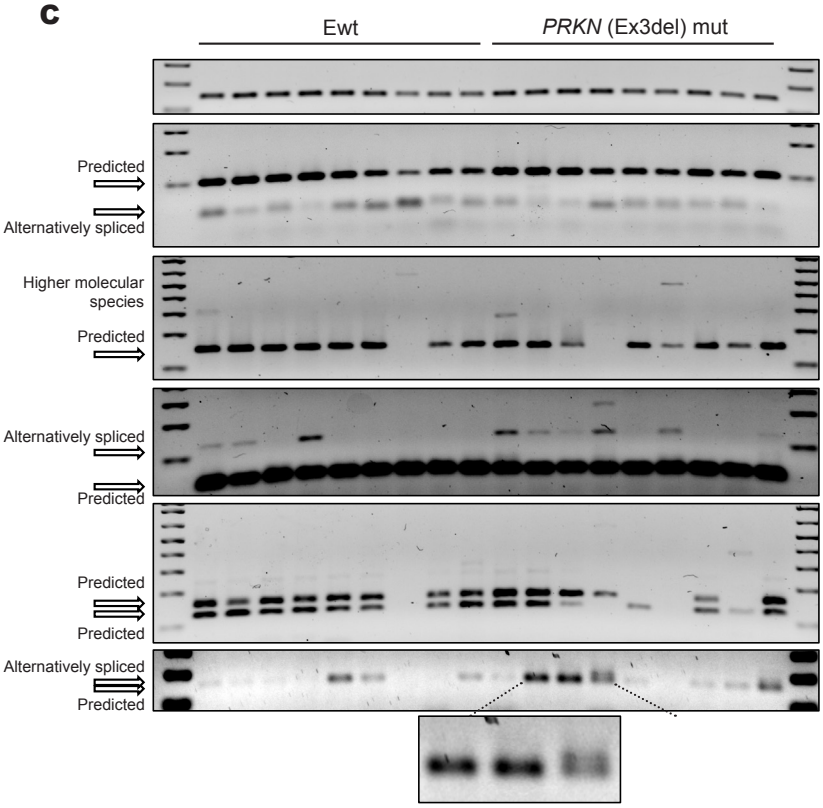

GAPDH - control

Region A
DDX46
DEAD Box Protein 46

Region B
DDX46

MARK4
Microtubule affinity regulating kinase 4
higher molecular weight species observed more in *PRKN* (Ex3del) mut

CAMSAP2
calmodulin regulated spectrin associated protein family member 2
Misregulation of *CAMSAP2* in *PRKN* (Ex3del) mut

MFSD6
Major Facilitator Superfamily Domain Containing 6
exon inclusion only observed in *PRKN* (Ex3del) mut